

Synthesis and Biological Evaluation (*in Vitro* and *in Vivo*) of Cyclic RGD Peptidomimetic - Paclitaxel Conjugates Targeting Integrin

Raffaele Colombo, Michele Mingozi, Laura Belvisi, Daniela Arosio, Umberto Piarulli, Nives Carenini, Paola Perego, Nadia Zaffaroni, Michelandrea De Cesare, Vittoria Castiglioni, Eugenio Scanziani, and Cesare Gennari

J. Med. Chem., **Just Accepted Manuscript** • Publication Date (Web): 09 Nov 2012

Downloaded from <http://pubs.acs.org> on November 9, 2012

Just Accepted

“Just Accepted” manuscripts have been peer-reviewed and accepted for publication. They are posted online prior to technical editing, formatting for publication and author proofing. The American Chemical Society provides “Just Accepted” as a free service to the research community to expedite the dissemination of scientific material as soon as possible after acceptance. “Just Accepted” manuscripts appear in full in PDF format accompanied by an HTML abstract. “Just Accepted” manuscripts have been fully peer reviewed, but should not be considered the official version of record. They are accessible to all readers and citable by the Digital Object Identifier (DOI®). “Just Accepted” is an optional service offered to authors. Therefore, the “Just Accepted” Web site may not include all articles that will be published in the journal. After a manuscript is technically edited and formatted, it will be removed from the “Just Accepted” Web site and published as an ASAP article. Note that technical editing may introduce minor changes to the manuscript text and/or graphics which could affect content, and all legal disclaimers and ethical guidelines that apply to the journal pertain. ACS cannot be held responsible for errors or consequences arising from the use of information contained in these “Just Accepted” manuscripts.



1
2
3
4
5
6
7
8
9
10
11
12
13
14
15
16
17
18
19
20
21
22
23
24
25
26
27
28
29
30
31
32
33
34
35
36
37
38
39
40
41
42
43
44
45
46
47
48
49
50
51
52
53
54
55
56
57
58
59
60

Synthesis and Biological Evaluation (*in Vitro* and *in Vivo*) of Cyclic RGD Peptidomimetic - Paclitaxel Conjugates Targeting Integrin $\alpha_V\beta_3$

Raffaele Colombo,[†] Michele Mingozi,[†] Laura Belvisi,[†] Daniela Arosio,[‡] Umberto Piarulli,^{*§}

Nives Carenini,[⊥] Paola Perego,[⊥] Nadia Zaffaroni,[⊥] Michelandrea De Cesare,[⊥] Vittoria

Castiglioni,^{||} Eugenio Scanziani,^{||} Cesare Gennari^{*†}

[†] Università degli Studi di Milano, Dipartimento di Chimica, via Golgi 19, I-20133, Milan, Italy

[‡] CNR, Istituto di Scienze e Tecnologie Molecolari (ISTM), via Golgi 19, I-20133, Milan, Italy

[§] Università degli Studi dell'Insubria, Dipartimento di Scienza e Alta Tecnologia, via Valleggio 11, I-22100, Como, Italy

[⊥] Molecular Pharmacology Unit, Dept. Experimental Oncology and Molecular Medicine, Fondazione IRCCS Istituto Nazionale Tumori, via Amadeo 42, I-20133 Milan, Italy

^{||} Università degli Studi di Milano, Dipartimento di Scienze Veterinarie e Sanità Pubblica, via Celoria 10, I-20133 Milan, Italy

1
2
3 **ABSTRACT.** A small library of integrin ligand - Paclitaxel conjugates **10-13** was synthesized
4
5 with the aim of using the tumor-homing *cyclo*[DKP-RGD] peptidomimetics for site-directed
6
7 delivery of the cytotoxic drug. All the Paclitaxel-RGD constructs **10-13** inhibited biotinylated
8
9 vitronectin binding to the purified $\alpha_v\beta_3$ integrin receptor at low nanomolar concentration and
10
11 showed *in vitro* cytotoxic activity against a panel of human tumor cell lines similar to that of
12
13 Paclitaxel. Among the cell lines, the cisplatin-resistant IGROV-1/Pt1 cells expressed high levels
14
15 of integrin $\alpha_v\beta_3$, making them attractive to be tested in *in vivo* models. *Cyclo*[DKP- β -RGD]-
16
17 PTX **11** displayed sufficient stability in physiological solution and in both human and murine
18
19 plasma to be a good candidate for *in vivo* testing. In tumor-targeting experiments against the
20
21 IGROV-1/Pt1 human ovarian carcinoma xenotransplanted in nude mice, compound **11** exhibited
22
23 a superior activity than Paclitaxel, despite the lower (ca. half) molar dosage used.
24
25
26
27
28
29
30

31 **INTRODUCTION**

32
33
34 Chemotherapy has been one of the main approaches for the treatment of cancer for more than
35
36 half a century and is based on the administration of drugs which often interfere with fundamental
37
38 cellular functions (e.g., DNA replication, cell division). The antitumor efficacy of anticancer
39
40 drugs is thus limited by their nonspecific toxicity to normal cells, especially to rapidly growing
41
42 cells such as blood, bone marrow and mucous membrane cells, resulting in a low therapeutic
43
44 index and serious side-effects. The efficacy of chemotherapy is further limited by the occurrence
45
46 or development of drug resistance: tumor cells can be regarded as a rapidly changing target
47
48 because of their genetic instability, heterogeneity, and high rate of mutation, leading to selection
49
50 and overgrowth of a drug-resistant tumor cell population.¹ In principle, the efficiency of the
51
52 treatment can be improved by increasing the doses, but this approach commonly results in severe
53
54 toxicity. Therefore, selective tumor targeting of chemotherapeutic agents represents a major goal,
55
56
57
58
59
60

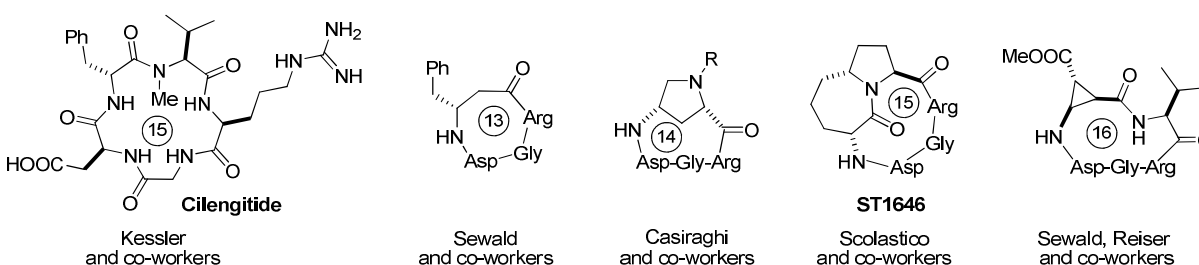
1
2
3 and various drug delivery systems have been recently developed,² including the use of
4 liposomes, microspheres, micelles, polymers, protein- or antibody-drug conjugates, and pro-
5 drugs.³ Considerable efforts are currently being made in this domain to such an extent that
6 leaders of major pharmaceutical companies foresee that >60% of all existing drugs will be
7 targeted in less than two decades.⁴ In this field, an attractive avenue for selective tumor targeting
8 are hybrid molecules designed to bind to specific over-expressed receptors on cancer cells.⁵
9
10 Clearly, the success of this approach is heavily dependent on the rational selection of appropriate
11 biological objectives.
12
13
14
15
16
17
18
19
20
21

22 Integrins are ideal pharmacological targets based on their key role in angiogenesis and tumor
23 development and on their easy accessibility as cell surface receptors interacting with
24 extracellular ligands.⁶ They are bidirectional glycoprotein heterodimeric receptors which connect
25 cells to the scaffolding proteins of the extracellular matrix, occurring in at least 24 pairs of 18 α
26 and 8 β subunits and containing large extracellular domains and short cytoplasmic domains.⁷
27 Integrins are also involved in tissue integrity and cell trafficking, growth, differentiation,
28 proliferation and migration.⁸ As a consequence of their role in so many fundamental processes,
29 integrin malfunction is connected to a large variety of diseases such as thrombosis, osteoporosis,
30 inflammation, and cancer.⁹ The tripeptide sequence arginine-glycine-aspartate (RGD) has been
31 identified as the common motif used by several endogenous ligands to recognize and bind a
32 group of integrins, including $\alpha_v\beta_3$, $\alpha_v\beta_5$, $\alpha_5\beta_1$, which are crucial in angiogenesis, tumor
33 progression and metastasis, and $\alpha_{IIb}\beta_3$, which is involved in platelet aggregation.¹⁰
34
35
36
37
38
39
40
41
42
43
44
45
46
47
48
49
50

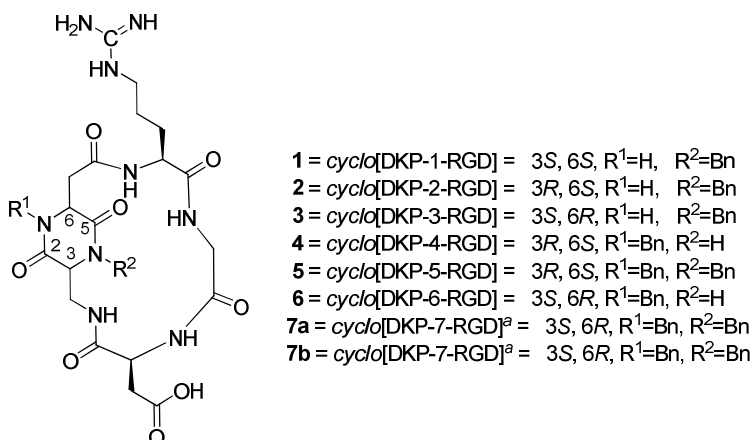
51 A potent $\alpha_v\beta_3$ integrin ligand, *cyclo*[Arg-Gly-Asp-D-Phe-N(Me)-Val] (Cilengitide) developed
52 by Kessler and co-workers (Figure 1),^{11,12} is currently in phase III clinical trials as an
53 angiogenesis inhibitor for patients with *glioblastoma multiforme*.¹³ The high activity and
54
55
56
57
58
59
60

selectivity of this derivative has been attributed to an extended conformation of the RGD motif displaying a distance of about 9 Å between the C_β atoms of Asp and Arg.^{12,14} These observations prompted many other research groups to investigate the use of conformationally constrained cyclic RGD peptidomimetics as active and selective integrin antagonists. A selection of these ligands, encompassing a wide variety of rigid scaffolds and featuring 13-, 14-, 15- and 16-membered rings, is shown in Figure 1.¹⁵

Figure 1. Potent $\alpha_v\beta_3$ integrin ligands



We have recently contributed to this field with a new class of cyclic RGD-peptidomimetics, containing bifunctional diketopiperazine (DKP) scaffolds and featuring 17-membered rings (Figure 2).¹⁶ The *cis*-derivative *cyclo*[DKP-1-RGD] (**1**) inhibited biotinylated vitronectin binding to the purified $\alpha_v\beta_3$ receptor at a micromolar concentration ($3.9 \pm 0.4 \mu\text{M}$), while *trans*-derivatives **2-7** ranged from submicro- to subnanomolar concentrations (220 - 0.2 nM).

Figure 2. Library of *cyclo*[DKP-RGD] integrin ligands

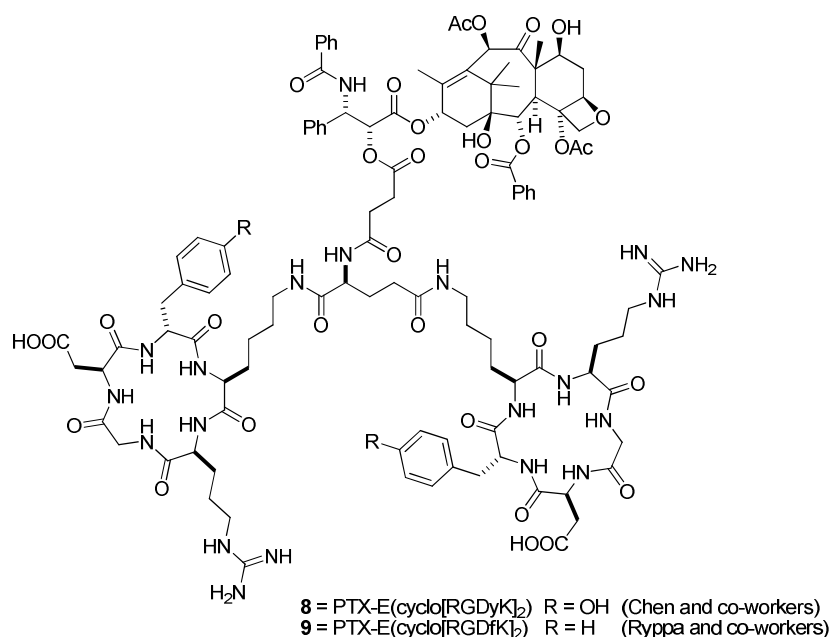
^a*N*-dibenzyl *cyclo*[DKP-7-RGD] was isolated as two different separable conformers (diastereomers, **7a** and **7b**) due to hindered rotation of one ring around the other, *i.e.*, the DKP *N*-benzyl group cannot pass inside the macrolactam ring, see ref. 16b.

It is now emerging that antiangiogenic therapy alone is not sufficient to fight and eradicate tumors: recent preclinical findings of a paradoxical pro-angiogenic activity of RGD-mimetic agents (like Cilengitide) at low concentrations have stimulated the debate on the use of antiangiogenetics as single drugs.¹⁷ Since α_v integrins, which can be internalized by cells, are involved in tumor angiogenesis and are overexpressed on the surface of cancer cells, integrin ligands can be usefully employed as tumor-homing peptidomimetics for site-directed delivery of cytotoxic drugs.¹⁸ During the past fifteen years, a number of RGD-cytotoxic drug conjugates have been developed. In these approaches, a few cyclic RGD integrin ligands (*e.g.*, RGD4C,¹⁹ *cyclo*[(NMe)VRGdf-NH],²⁰ *cyclo*[RGdfK],^{21,22} *cyclo*[CRGDC],²² *cyclo*[RGdf-Aad],^{23a} *cyclo*[RGdf-Amp]^{23a}) were conjugated to a cytotoxic drug (*e.g.*, doxorubicin,^{19,21} doxsaliform,²⁰ camptothecin,^{23a,b} cisplatin²²) through different linkers, such as amides,^{19,22,23a} oximes,^{20,23a} maleimides,²¹ carbamates,^{23b} and hydrazones.^{23a} Notably, Chen and co-workers prepared the RGD ligand - Paclitaxel conjugate **8** (Figure 3), which was covalently assembled by joining the

1
2
3
4
5
6
7
8
9
10
11
12
13
14
15
16
17
18
19
20
21
22
23
24
25
26
27
28
29
30
31
32
33
34
35
36
37
38
39
40
41
42
43
44
45
46
47
48
49
50
51
52
53
54
55
56
57
58
59
60

microtubule-stabilizing anticancer agent to the dimeric RGD peptide E[*cyclo*(RGDyK)]₂ via a cleavable succinyl ester linker, and evaluated its antitumor activity on the metastatic breast cancer cell line MDA-MB-435.²⁴ In mice, conjugate **8** showed a moderately improved antitumor effect over Paclitaxel, but no tumor regression could be observed. The stability of the succinyl linker was not assessed and a premature release of Paclitaxel can be suspected.

Figure 3. Dimeric RGD ligand - Paclitaxel conjugates

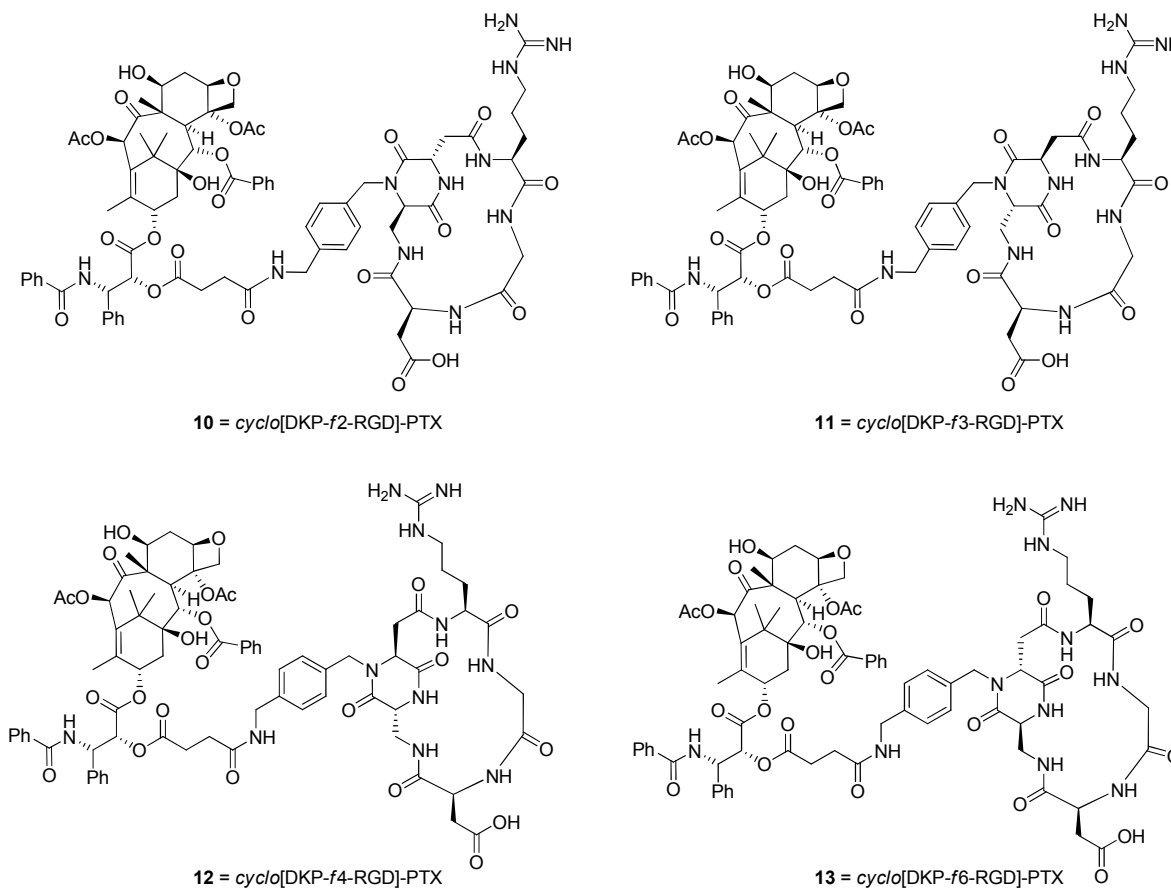


A very similar conjugate (*i.e.*, compound **9** reported in Figure 3) was extensively evaluated in a recent study by Ryppa and co-workers on an ovarian carcinoma xenograft model (OVCAR-3).²⁵ Although the construct provided promising results *in vitro*, unfortunately it did not show any antitumor effect *in vivo*. The stability of conjugate **9** in a glucose phosphate buffer solution at pH=7 was studied over 24 h, yielding a half-life of only ~2 h at 37 °C. Half-life in the bloodstream is expected to be much shorter, and the inefficacy of this conjugate was attributed to

1
2
3 hydrolysis of the ester bond at the 2' position of Paclitaxel, which causes premature release of
4
5 the cytotoxic agent and loss of the tumor-homing effect.
6
7

8 Herein, we present a full account of our investigations reporting: (i) the synthesis of new
9
10 *cyclo*[DKP-RGD] integrin ligands, bearing a free amine group suitable for conjugation to a
11
12 cytotoxic drug; (ii) the conjugation of these ligands to Paclitaxel via a succinyl linker to give
13
14 *cyclo*[DKP-RGD] - Paclitaxel conjugates **10-13** (Figure 4); (iii) the stability of a *cyclo*[DKP-
15
16 RGD] - Paclitaxel construct in a physiological solution and in both human and murine plasma,
17
18 which turned out to be far better than the case reported above;²⁵ (iv) the ability of the
19
20 *cyclo*[DKP-RGD] - Paclitaxel conjugates to compete with biotinylated vitronectin for binding to
21
22 the purified $\alpha_v\beta_3$ and $\alpha_v\beta_5$ receptors; (v) *in vitro* cytotoxic activity of the *cyclo*[DKP-RGD] -
23
24 Paclitaxel conjugates in a panel of human cancer cell lines; (vi) *in vivo* tumor-targeting efficacy
25
26 against the IGROV-1/Pt1 human ovarian carcinoma xenotransplanted in nude mice; (vii) the
27
28 effects of tumor treatment, analyzed using immunohistochemistry.
29
30
31
32
33
34
35
36
37
38
39
40
41
42
43
44
45
46
47
48
49
50
51
52
53
54
55
56
57
58
59
60

Figure 4. Structure of *cyclo*[DKP-RGD] - Paclitaxel conjugates **10-13**



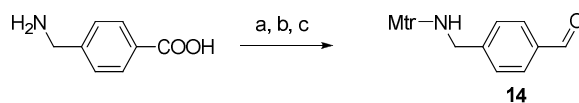
RESULTS AND DISCUSSION

Synthesis. In order to prepare cyclic RGD-peptidomimetics covalently linked to Paclitaxel (compounds **10-13**, Figure 4), four functionalized (*f*) *trans* diketopiperazines (*i.e.*, DKP-*f*2, DKP-*f*3, DKP-*f*4, DKP-*f*6) were synthesized, varying the position of the *p*-aminomethylbenzyl *N*-substituent (*N*-1 or *N*-4) and the absolute stereochemistry at C-3 and C-6 (Schemes 1-3). These DKPs were used for the synthesis of *cyclo*[DKP-RGD] integrin ligands (Scheme 4), which were conjugated to 2'-succinyl Paclitaxel (Scheme 5).

For the preparation of the functionalized *trans* diketopiperazines DKP-*f*2, DKP-*f*3, DKP-*f*4, and DKP-*f*6, we selected a linker bearing both an aldehyde (for successive reductive alkylation)

and an amino group (for the final conjugation to Paclitaxel). Thus, linker **14** was synthesized in three steps from 4-aminomethyl benzoic acid via LiAlH₄ reduction, primary amine protection as 4-methoxy-2,3,6-trimethylbenzenesulphonamide (Mtr) and benzylic alcohol oxidation using activated MnO₂ (Scheme 1). The Mtr protecting group was chosen because of its stability and orthogonality with the methyl, benzyl, allyl, *t*Bu, Boc, and Cbz protecting groups.

Scheme 1. Synthesis of aldehyde **14**^a

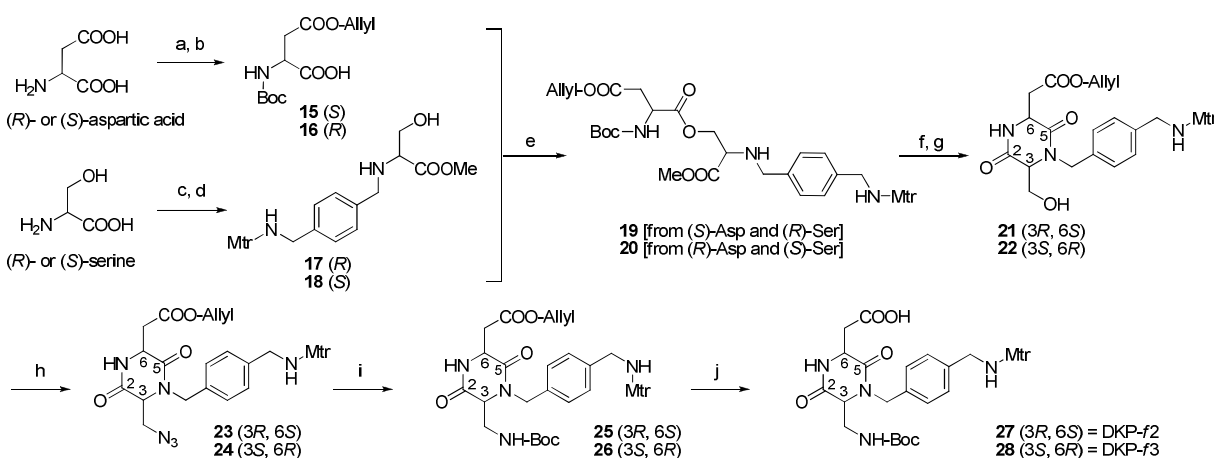


^aReagents and conditions: (a) LiAlH₄, THF, 8 h, reflux, 70%; (b) Mtr-Cl, *i*-Pr₂NEt, THF, 6 h, room temp., 85%; (c) MnO₂, THF, overnight, room temp., quant..

Trans scaffolds DKP-*f*2, DKP-*f*3 (Scheme 2) and DKP-*f*4, DKP-*f*6 (Scheme 3) were synthesized starting from commercially available (*R*)- or (*S*)-aspartic acid and (*R*)- or (*S*)-serine. Two different synthetic strategies were developed depending on the nitrogen substitution. In particular, the synthesis of DKP-*f*2 and DKP-*f*3 (bearing the linker on DKP nitrogen *N*-4, former serine nitrogen) was realized making use of a serine ligation strategy,²⁶ as described in Scheme 2. (*R*)- and (*S*)-Aspartic acid were initially protected as allyl ester on the side chain and as *N*-Boc to give the enantiomeric derivatives (*S*)-**15** and (*R*)-**16**. (*R*)- and (*S*)-Serine were protected as methyl ester and reductively alkylated with aldehyde **14** and sodium triacetoxyborohydride to afford the enantiomeric compounds (*R*)-**17** and (*S*)-**18**. Direct coupling (HATU, *i*Pr₂NEt) of protected aspartic acid (*S*)-**15** with functionalized serine (*R*)-**17**, or of the enantiomers (*R*)-**16** with (*S*)-**18**, led to the isopeptides (*S,R*)-**19** and (*R,S*)-**20** in high yield (86%), rather than forming the expected dipeptides. The *O,N*-acyl migration²⁶ was then triggered by cleavage of the Boc protecting group and treatment with a base (*i*Pr₂NEt) in a protic solvent (*i*PrOH), which also

promoted the simultaneous cyclization to the *trans* diketopiperazines **21** and **22** (93% overall yield). The hydroxyl group of **21** and **22** was converted into azides **23** and **24** via a Mitsunobu reaction in good yield (86%), using $\text{HN}_3 \cdot \text{Tol}$ in a toluene / dichloromethane solution. Finally, a one-pot Staudinger reduction - Boc protection, followed by allyl deprotection yielded the *trans* scaffolds DKP-*f*2 (**27**; 3*R*,6*S*) and DKP-*f*3 (**28**; 3*S*,6*R*) in 88% yield. This synthetic route involves a high overall yield (60%) and only a few chromatographic purifications, which allows easy preparation on a multi-gram scale.

Scheme 2. Synthesis of DKP-*f*2 and DKP-*f*3^{a,b}

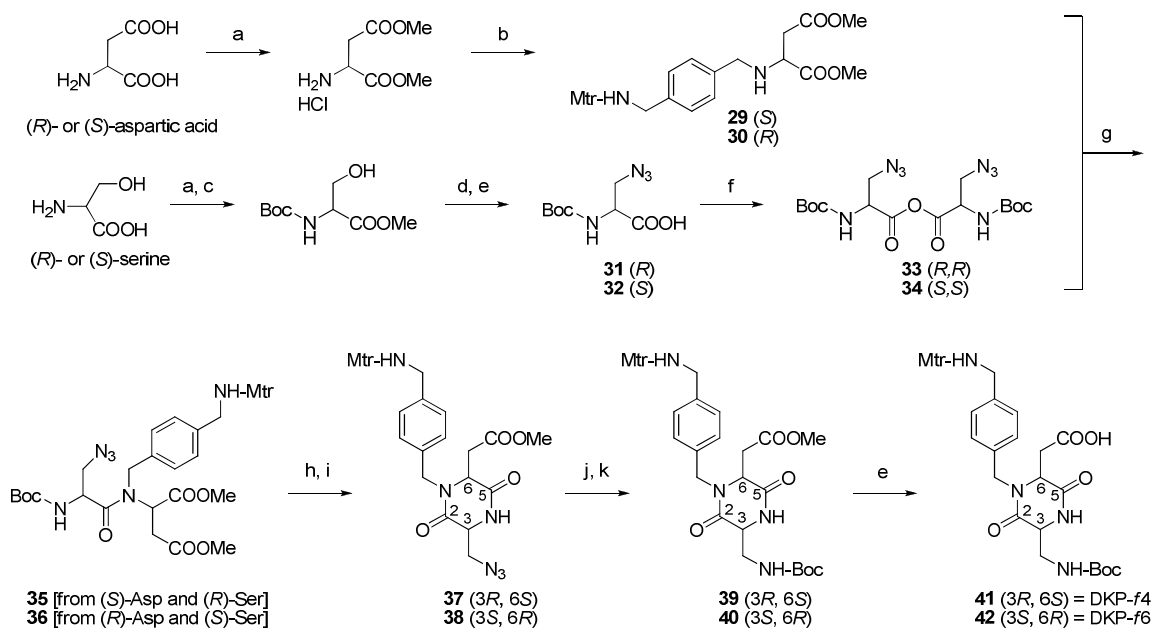


^aReagents and conditions: (a) allyl alcohol, AcCl ; (b) Boc_2O , TEA, Dioxane, water, 95% over two steps; (c) MeOH, AcCl , quant.; (d) aldehyde **14**, $\text{NaBH}(\text{OAc})_3$, THF, 3 h, room temp., quant.; (e) HATU, HOAT, $i\text{Pr}_2\text{NEt}$, DMF, 3 h, 0 °C to room temp., 86%; (f) TFA/DCM 1:2, 3 h, 0 °C to room temp.; (g) $i\text{Pr}_2\text{NEt}$, $i\text{PrOH}$, 6 h, room temp., 93% over two steps; (h) $\text{HN}_3 \cdot \text{Tol}$, DIAD, Ph_3P , DCM/Tol 1:2, 7 h, -20 °C, 86%; (i) Me_3P , BOC-ON, THF, 6 h, -20 °C to room temp., 88%; (j) pyrrolidine, PPh_3 , $[\text{Pd}(\text{PPh}_3)_4]$, DCM, 4 h, room temp., quant.. ^bYields reported are the average of six experiments, including different reaction batches with the two enantiomeric products.

For the synthesis of *trans* scaffolds DKP-*f*4 and DKP-*f*6 (Scheme 3), (R)- and (S)-aspartic acid were protected as dimethyl ester and reductively alkylated with aldehyde **14** to obtain the enantiomeric derivatives (S)-**29** and (R)-**30**. The hydroxyl group of (R)- or (S)-Boc-Ser-OMe was

1
2
3 first transformed into the corresponding azide under Mitsunobu conditions in 78% yield and then
4
5 the methyl ester was saponified. The resulting enantiomeric acids (*R*)-**31** and (*S*)-**32**, stable only
6
7 for a few hours, were immediately self-condensed with DCC in DCM to give the symmetric
8
9 anhydrides (*R,R*)-**33** and (*S,S*)-**34**, which were isolated by filtering off the *N,N'*-dicyclohexylurea
10
11 (DCU) and immediately reacted with the functionalized aspartic acid dimethylester (*S*)-**29** or (*R*)-
12
13 **30** to obtain the enantiomeric dipeptides (*S,R*)-**35** and (*R,S*)-**36** in moderate yield (40%). Yield
14
15 optimization was pursued by extensively varying the reaction conditions (equivalents, solvents,
16
17 temperature, time) but all the attempts were not successful, and markedly differed from the
18
19 analogous reaction run on *N*-benzyl-aspartic acid dimethylester (i.e. **29** or **30** missing the Mtr-
20
21 NH-CH₂- side chain) where the yield was uniformly higher (80%).^{16b} All other coupling reagents
22
23 tested (HATU, PyBrOP, DPPA, etc.) were ineffective for this reaction; although no coupling
24
25 product of the dehydroalanine derivative was ever detected, the beta-elimination possibly caused
26
27 by excess *i*Pr₂NEt in the HATU, PyBrOP and DPPA tentative couplings might be an additional
28
29 reason for this failure, combined with the poor reactivity of the sterically hindered secondary
30
31 amine of the aspartic derivative.
32
33
34
35
36
37

38
39 After Boc deprotection, the six-membered cyclization occurred spontaneously with 4 equiv of
40
41 *i*Pr₂NEt in *i*PrOH, to give diketopiperazines (*3R,6S*)-**37** and (*3S,6R*)-**38** in 92% yield. *Trans*
42
43 scaffolds DKP-*f*4 (**41**; *3R,6S*) and DKP-*f*6 (**42**; *3S,6R*) were finally obtained by catalytic
44
45 hydrogenation of the azide, Boc protection of the primary amine and hydrolysis of the methyl
46
47 ester (96% overall yield).
48
49
50
51
52
53
54
55
56
57
58
59
60

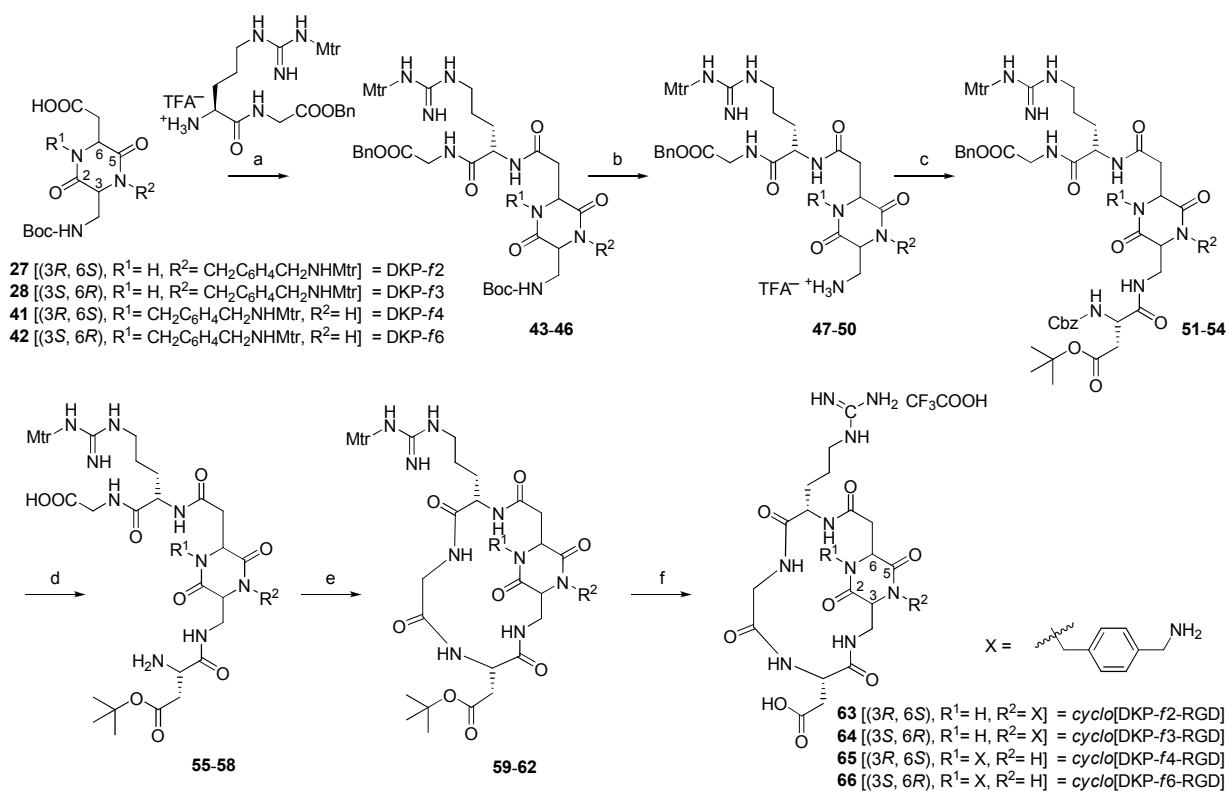
Scheme 3. Synthesis of DKP-*f4* and DKP-*f6*^{a,b}

^aReagents and conditions: (a) MeOH, AcCl, quant.; (b) aldehyde **14**, NaBH₃(CN), MeOH, 4 h, room temp., 66%; (c) Boc₂O, TEA, dioxane-water, 95%; (d) HN₃·Tol, DIAD, Ph₃P, THF, 7 h, -20 °C, 78%; (e) LiOH, H₂O/THF 1:1, 1 h, 0 °C, quant.; (f) DCC, DCM, 1 h, room temp., quant.; (g) DCM, overnight, room temp., 40%; (h) TFA, Et₃SiH, DCM, 3 h, room temp., quant.; (i) *i*Pr₂NEt, *i*PrOH, 6 h, room temp., 92%; (j) H₂, 10% Pd/C, THF, 4 h, room temp., quant.; (k) Boc₂O, *i*Pr₂NEt, DCM, 6 h, room temp., 96%. ^bYields reported are the average of six experiments, including different reaction batches with the two enantiomeric products.

Trans diketopiperazines DKP-*f2*, DKP-*f3*, DKP-*f4* and DKP-*f6* were used as scaffolds for the synthesis of functionalized *cyclo*[DKP-RGD] integrin ligands **63-66**, following a solution-phase strategy (Scheme 4). Dipeptide Boc-Arg(Mtr)-Gly-OBn, prepared on a multigram scale following our reported procedure,^{16b} was Boc-deprotected and coupled to the chosen diketopiperazine scaffold to give compounds **43-46** in good yields (83-85%). The Boc protecting group of compounds **43-46** was then removed and the resulting free amines **47-50** were coupled to Cbz-Asp(OtBu)-OH to obtain the linear Cbz-Asp(OtBu)-DKP-Arg(Mtr)-Gly-OBn peptidomimetics **51-54** in high yields (86-88%). After carboxybenzyl and benzyl groups simultaneous deprotection by catalytic hydrogenolysis to give **55-58** quantitatively, the synthesis

of protected *cyclo*(DKP-RGD) **59-62** was accomplished in good yield (60-81%) by 17-membered macrolactamization in a highly diluted DMF solution (1.4 mM) utilizing HATU, HOAT, *i*-Pr₂NEt (4:4:6 equiv). The final step was the non trivial removal of the side chain protecting groups.

Scheme 4. Synthesis of functionalized *cyclo*[DKP-RGD] integrin ligands **63-66**^a



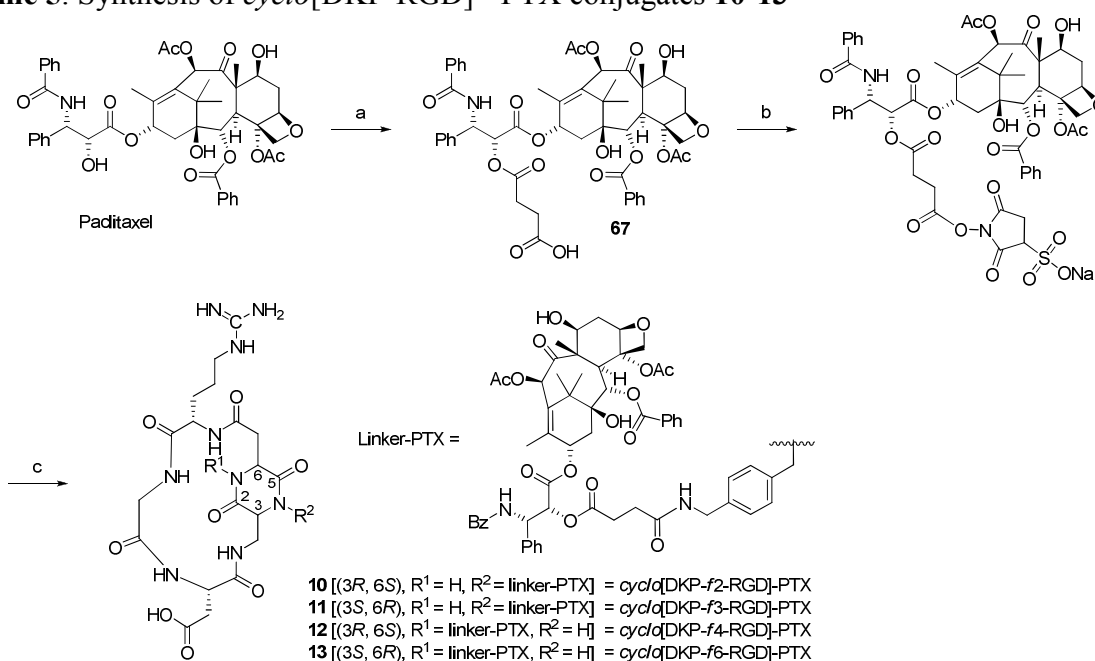
^aReagents and conditions: (a) HATU, HOAT, *i*Pr₂NEt, DMF, overnight, room temp., 83-85%; (b) TFA/DCM 1:2, 3 h, room temp., quant.; (c) Cbz-Asp(OtBu)-OH, HATU, HOAT, *i*Pr₂NEt, DMF, overnight, room temp., 86-88%; (d) H₂, 10% Pd/C, THF/H₂O 1:1, overnight, room temp., quant.; (e) HATU, HOAT, *i*Pr₂NEt, 1.4 mM in DMF, overnight, room temp., 60-81%; (f) TFA/TMSBr/thioanisole/EDT/phenol 70:14:10:5:1, 2 h, room temp., 70-85%.

The OtBu and the Mtr on the arginine were easily deprotected while the Mtr on the benzylic amine was very stable. Several cleavage cocktails were screened and the more classic²⁷ [“Reagent K” (TFA/phenol/water/TIPS, 88/5/5/2), “Reagent R” (TFA/thioanisole/EDT/anisole,

90/5/3/2) and “Reagent P+” (TFA/phenol/methanesulfonic acid, 95/2.5/2.5)] failed, giving the mono-protected compound as main product (the Mtr on the amine was still present), with a low yield (5-20%) of the desired totally deprotected product, even after 48 h. Finally, with the use of TFA/TMSBr/thioanisole/EDT/phenol (70/14/10/5/1) cleavage cocktail at room temperature for 2 h, fully deprotected compounds **63-66** were obtained in 70-85% isolated yield.

Thus, we were ready to conjugate Paclitaxel to our ligands: the 2'-hydroxyl function of Paclitaxel was derivatized with succinic anhydride, following a reported procedure.²⁸ The resulting Paclitaxel hemisuccinate ester **67**²⁸ was activated using diisopropylcarbodiimide (DIC) and *N*-hydroxysulfosuccinimide sodium salt (sulfo-NHS), followed by coupling with *cyclo*[DKP-RGD] ligands **63-66** (Scheme 5).

Scheme 5. Synthesis of *cyclo*[DKP-RGD] - PTX conjugates **10-13**^a

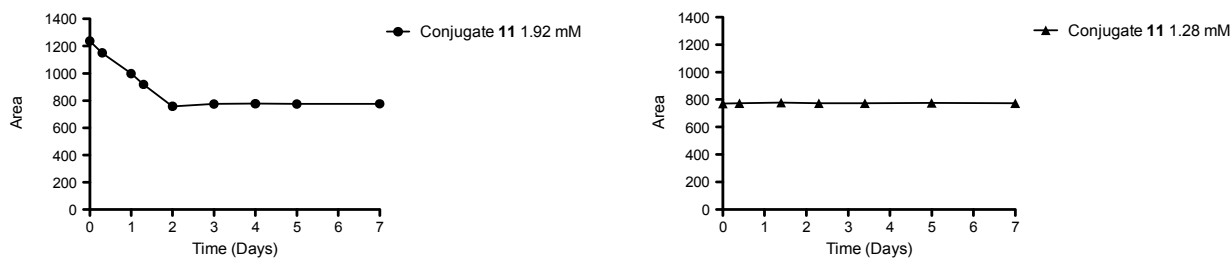


^aReagents and conditions: (a) succinic anhydride, py, DCM, overnight, 0 °C to room temp., 94%; (b) *N*-hydroxysulfosuccinimide sodium salt, DIC, DMF, overnight, room temp.; (c) *cyclo*(DKP-RGD) **63**, **64**, **65** or **66**, CH₃CN, aq. phosphate buffer, pH = 7.3, 10 h at 0 °C then 8 h at room temp., 60-70%.

The conjugation yield was strongly pH-dependent: at pH < 7.0 the reaction did not proceed, whereas at pH > 7.5 the hydrolysis of the sulfo-NHS ester substantially competed with the primary amine reaction. The synthesis of conjugates **10-13** was finally achieved in good yield (60-70%) by adding a 0.1 M aqueous NaOH solution when required throughout the reaction, for maintaining the pH value at 7.3.

Solubility and stability in a physiological solution. The solubility of conjugate *cyclo*[DKP- β -RGD]-PTX **11** was investigated in a physiological solution (0.9% NaCl in H₂O)/Cremophor EL/ethanol (90:5:5 v/v) by quantitative HPLC. A 1.92 mM clear solution turned out to be oversaturated and slowly flocculated to reach a concentration of 1.28 mM in 2 days (Figure 5, left diagram). The precipitate was the conjugate **11** itself, with a purity > 99.5%. Compound **11** (1.28 μ mol) dissolved in 0.1 mL of Cremophor EL/ethanol (1:1 v/v) and diluted with 0.9 mL of physiological solution, was perfectly stable for one week, with a purity > 99.5%. The 1.28 mM solution did not undergo any precipitation or decomposition (Figure 5, right diagram).

Figure 5. Solubility and stability of *cyclo*[DKP- β -RGD]-PTX **11** in a physiological solution^a

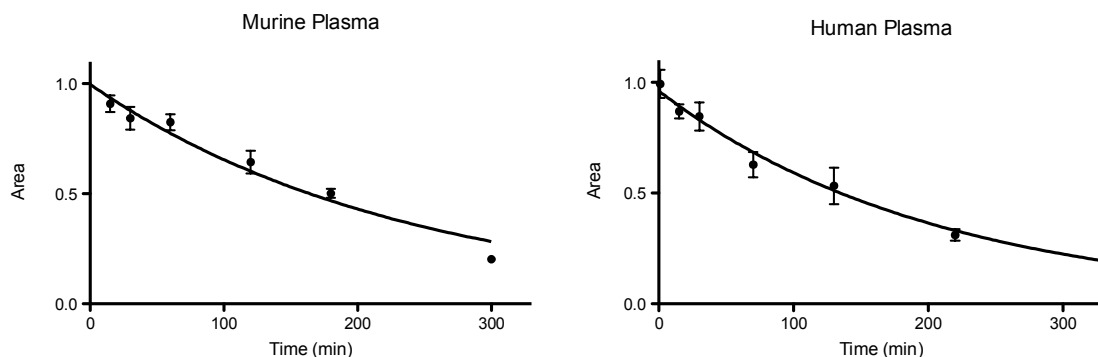


^aQuantitative HPLC determination of solubility and stability of compound **11** in a physiological solution (0.9% NaCl in H₂O)/Cremophor EL/ethanol (90:5:5 v/v). A 1.92 mM clear solution of **11** turned out to be oversaturated and slowly flocculated to reach a concentration of 1.28 mM in 2 days (left diagram). The 1.28 mM solution did not undergo any precipitation or decomposition over seven days (right diagram).

1
2
3
4
5 **Plasma stability assays.** Paclitaxel conjugate **11** (1.28 μmol) was dissolved in DMSO (128
6 μL) and then diluted with pH 7.5 phosphate buffer (PBS) to give a 200 μM stock solution.
7
8 Murine plasma was spiked with the stock solution to obtain a final 10 μM concentration and
9
10 incubated at 37 $^{\circ}\text{C}$. At time points varying from 1 min to 330 min, aliquots of 50 μL were taken
11
12 and quenched with 200 μL of ice-cold acetonitrile (containing Verapamil as internal standard,
13
14 see the Experimental Section for details). Samples were centrifuged at 3000 rpm for 20 min and
15
16 the supernatant was analyzed by RP-HPLC UV-MS/MS. The data were fitted using a signal
17
18 phase exponential decay and the calculated half-life was = 165 ± 2 min (Figure 6, left diagram).
19
20 The same procedure was adopted for a pooled human plasma stability assay and in this case the
21
22 calculated half-life was = 143 ± 3 min (Figure 6, right diagram). Free Paclitaxel accumulated
23
24 during the assays as a result of hydrolysis of the succinyl ester bond at the PTX-2' position.
25
26 These results were very encouraging and showed that *cyclo*[DKP- β -RGD]-PTX **11** is
27
28 sufficiently stable to undergo animal testing with murine models. In fact, similar RGD ligands
29
30 showed significant (maximum) tumor uptakes *in mice* after 10,²⁹ 20,³⁰ 30,³¹ and 60 min.³²
31
32

33
34
35
36
37
38
39 Summarizing, we have investigated the stability of compound **11** to hydrolysis both in a
40
41 physiological solution and in murine and human plasma. As a matter of fact, *cyclo*[DKP- β -
42
43 RGD]-PTX **11** turned out to be far more stable than PTX-E[*cyclo*(RGDfK)]₂ **9**²⁵ (see Figure 3,
44
45 and the relevant discussion in the Introduction). The rather high stability of **11** can possibly be
46
47 attributed to a more lipophilic structure, where the ester linkage is less accessible in the protic
48
49 medium than in Ryppa's compound **9**.
50
51
52
53
54
55
56
57
58
59
60

Figure 6. Stability of *cyclo*[DKP- β 3-RGD]-PTX **11** in murine and human plasma^a



^aQuantitative HPLC determination of stability of compound **11** (10 μ M) in murine plasma (left diagram) and in human plasma (right diagram) at 37 $^{\circ}$ C.

Integrin receptors competitive binding assays. *Cyclo*[DKP-RGD] - PTX conjugates **10-13** were examined *in vitro* for their ability to inhibit biotinylated vitronectin binding to the purified $\alpha_v\beta_3$ and $\alpha_v\beta_5$ receptors and compared to their unfunctionalized analogs **2, 3, 4** and **6**, to the unconjugated ligands **64** and **68**, and to the reference compounds *cyclo*[RGDFV]³³ and ST1646.³⁴ The results are collected in Table 1. Screening assays were performed incubating the immobilized integrin receptors with various concentrations (10^{-12} - 10^{-5} M) of the RGD ligands in the presence of biotinylated vitronectin (1 μ g/mL), and measuring the concentration of bound vitronectin in the presence of the competitive ligands. Low nanomolar values were obtained with all the Paclitaxel-RGD constructs (**10-13**), comparable to the unfunctionalized ligands (**2, 3, 4** and **6**). These data reassured us that the enormous increase of steric hindrance in the *cyclo*[DKP-RGD] - PTX conjugates, due to presence of the linker bearing Paclitaxel through the succinate tether, did not influence the high affinity for integrin receptors $\alpha_v\beta_3$ and $\alpha_v\beta_5$. Notably, for inhibition of vitronectin binding to the $\alpha_v\beta_3$ receptor, unconjugated ligand **64** required a 5-fold higher concentration than both its unfunctionalized and conjugated analogs (compounds **3** and

11, respectively). This reduced affinity may result from perturbation of the electrostatic clamp (*i.e.* the binding interactions of the carboxylate and guanidinium groups with the charged regions of the receptor),¹⁴ induced by the free amine present in **64**.

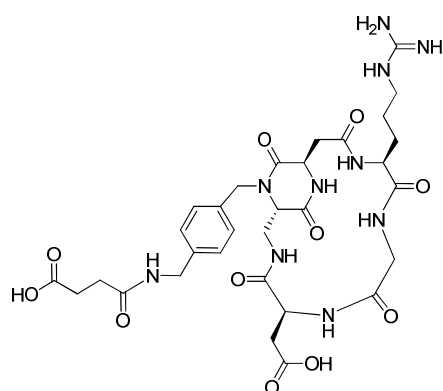
Table 1. Inhibition of biotinylated vitronectin binding to $\alpha_v\beta_3$ and $\alpha_v\beta_5$ receptors

Compound	Structure	$\alpha_v\beta_3$ IC ₅₀ [nM] ^a	$\alpha_v\beta_5$ IC ₅₀ [nM] ^a
10	<i>cyclo</i> [DKP- <i>f</i> ₂ -RGD]-PTX ^b	8.5 ± 0.8	518 ± 10
11	<i>cyclo</i> [DKP- <i>f</i> ₃ -RGD]-PTX ^b	5.2 ± 2.3	219 ± 124
12	<i>cyclo</i> [DKP- <i>f</i> ₄ -RGD]-PTX ^b	0.9 ± 0.6	76 ± 32
13	<i>cyclo</i> [DKP- <i>f</i> ₆ -RGD]-PTX ^b	1.1 ± 0.1	22 ± 3
64	<i>cyclo</i> [DKP- <i>f</i> ₃ -RGD] ^c	26.4 ± 3.7	> 5·10 ³
68	<i>cyclo</i> [DKP- <i>f</i> ₃ -RGD]- hemisuccinamide ^d	4.1 ± 0.6	75 ± 1
2	<i>cyclo</i> [DKP-2-RGD] ^e	3.2 ± 2.7	114 ± 99
3	<i>cyclo</i> [DKP-3-RGD] ^e	4.5 ± 1.1	149 ± 25
4	<i>cyclo</i> [DKP-4-RGD] ^e	7.6 ± 4.3	216 ± 5
6	<i>cyclo</i> [DKP-6-RGD] ^e	2.1 ± 0.6	79 ± 3
<i>cyclo</i> [RGDfV] ^f	<i>cyclo</i> [RGDfV]	3.2 ± 1.3	7.5 ± 4.8
ST1646 ^f	ST1646 ^g	1.0 ± 0.5	1.4 ± 0.8

^aIC₅₀ values were calculated as the concentration of compound required for 50% inhibition of biotinylated vitronectin binding as estimated by GraphPad Prism software; all values are the arithmetic mean ± SD of triplicate determinations. ^bSee Figure 4. ^cSee Scheme 4. ^dCompound **68** (see Figure 7) was synthesized as described in the Supporting Information. ^eSee Figure 2. ^fReference compound. ^gSee Figure 1.

Derivatization of the amine with succinic anhydride gave the hemisuccinamide **68** and restored the high binding affinity for the $\alpha_v\beta_3$ receptor. Interestingly, unlike reference compounds *cyclo*(RGDfV) and ST1646, the *cyclo*[DKP-RGD] peptidomimetics were ca. 20-200 fold more selective for the $\alpha_v\beta_3$ integrin with respect to the $\alpha_v\beta_5$ in this kind of assay.

Figure 7. *Cyclo*[DKP- β 3-RGD] - hemisuccinamide



68 = *cyclo*[DKP- β 3-RGD]-hemisuccinamide

Sensitivity of tumor cell lines treated with *cyclo*[DKP-RGD] - PTX conjugates 10-13.

Cyclo[DKP-RGD] - PTX conjugates **10-13** were tested *in vitro* for their cytotoxic activity in comparison with Paclitaxel, against a panel of human tumor cell lines. The cell sensitivity assays (Table 2) clearly indicated that the functionalized *cyclo*[DKP- β 3-RGD] integrin ligand **64** was not cytotoxic, while the *cyclo*[DKP-RGD]-PTX conjugates displayed a cytotoxic activity similar to that of Paclitaxel (same order of magnitude). These data imply that free Paclitaxel is released at some stage, possibly after the conjugates have been internalized into the cells, because it is well known that the free 2'-OH group is necessary for Paclitaxel to exert its cytotoxic and microtubule-stabilizing activities.³⁵ Compounds **10-13**, **64** and Paclitaxel were also tested *in vitro* on normal HDFC fibroblasts. When cells started to proliferate and were exposed to different

concentrations of these compounds (range of concentrations tested = 64-1000 nM), a marginal inhibition of cell growth was observed. The effect was not concentration-dependent, suggesting that the compounds were not cytotoxic but were at best cytostatic in these cells. The data reported in Table 2 did not identify undoubtedly a lead compound for evaluation of antitumor activity with *in vivo* models. Therefore, we chose *cyclo*[DKP-*f*3-RGD]-PTX **11** as our lead conjugate mainly because of its straightforward synthetic accessibility on a multi-gram scale.

Flow cytometry was used to detect the expression of $\alpha_v\beta_3$ and $\alpha_v\beta_5$ integrins on the surface of the different cancer cell lines (Table 3). Among these, the cisplatin-resistant IGROV-1/Pt1 cells expressed very high levels of integrin $\alpha_v\beta_3$, making them attractive to be tested in murine models with *cyclo*[DKP-RGD]-PTX construct **11** (*vide infra* the *in vivo* experiments).

Table 2. Cell sensitivity of different tumor cell lines to compounds **10-13** and **64**^a

Compd	Structure	IC ₅₀ (nM)					
		IGROV-1	IGROV-1/Pt1	U2-OS	SKOV3	PANC-1	MIA-PaCa2
10	<i>Cyclo</i> [DKP- <i>f</i> 2-RGD]-PTX	17.7 ± 6.0	18.7 ± 6.0	2.2 ± 0.5	1.6 ± 1.0	5.8 ± 4.0	2.0 ± 0.7
11	<i>Cyclo</i> [DKP- <i>f</i> 3-RGD]-PTX	61.3 ± 19.1	4.9 ± 2.0	12.8 ± 0.1	1.2 ± 0.1	2.4 ± 0.8	2.3 ± 0.4
12	<i>Cyclo</i> [DKP- <i>f</i> 4-RGD]-PTX	34.4 ± 29.0	3.7 ± 2.0	6.8 ± 4.6	2.4 ± 0.9	3.2 ± 0.7	1.8 ± 0.6
13	<i>Cyclo</i> [DKP- <i>f</i> 6-RGD]-PTX	48.2 ± 2.2	2.4 ± 1.9	5.7 ± 4.4	2.4 ± 1.1	3.5 ± 0.1	2.5 ± 0.6
64	<i>Cyclo</i> [DKP- <i>f</i> 3-RGD]	> 1200	> 18000	> 6300	> 11600	> 11600	> 11600
PTX	Paclitaxel	23.0 ± 0.8	2.2 ± 0.8	3.4 ± 0.4	2.7 ± 1.1	5.2 ± 1.9	7.2 ± 3.8

^aCell sensitivity was evaluated by growth inhibition assays based on cell counting. Cells were seeded and 24 h later they were exposed to the compounds for 72 h. At the end of treatment, cells were counted using a cell counter.

Table 3. Integrin expression of tumor cell lines of different tumor types^a

Integrin	Mean fluorescence intensity					
	IGROV-1	IGROV-1/Pt1	U2-OS	SKOV3	PANC-1	MIA-PaCa2
$\alpha_v\beta_3$	4.8 ± 1.9	23.3 ± 5.0	1.8 ± 0.6	6.4 ± 0.05	7.9 ± 2.8	1.2 ± 0.1
$\alpha_v\beta_5$	3.4 ± 0.9	3.3 ± 0.5	27.4 ± 0.1	4.4 ± 0.5	25.7 ± 6.5	5.6 ± 0.9

^aIntegrin expression levels were examined by immunofluorescence using a flow cytometer. The ratios between the mean fluorescence intensity of cells incubated with primary antibody and isotypic control are shown.

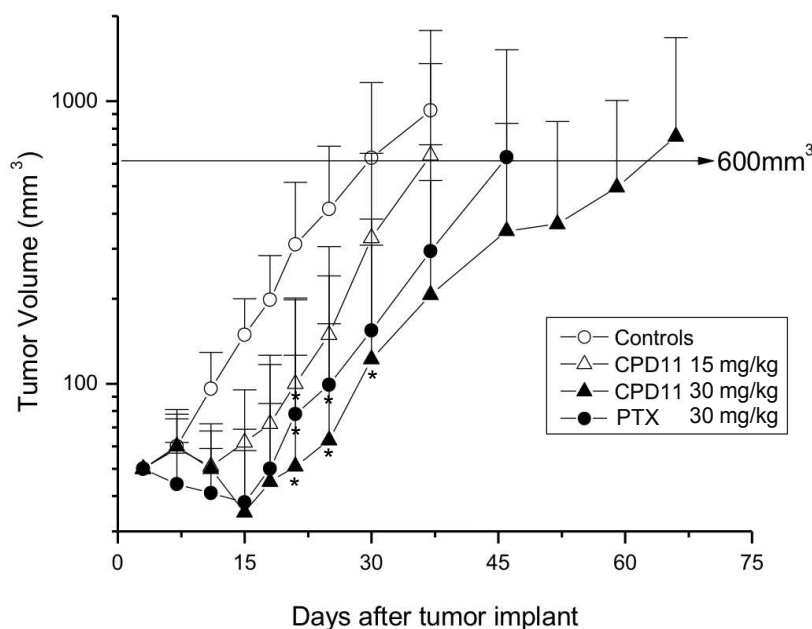
Comparing the data presented in Tables 2 and 3, it is quite clear that there is no correlation between the phenotypic integrin expression levels and efficacy of *cyclo*[DKP-RGD]-PTX conjugates, in *in vitro* assays. The cell sensitivity studies were carried out to determine whether Paclitaxel was released from the conjugate; in these *in vitro* assays, no tumor homing effect can be expected and therefore the different response can be attributed only to a higher or lower sensitivity of the different cell lines to the particular compound tested, independently of the integrin receptor expression. On the other hand, the evaluation of integrin expression was important for the choice of the best *in vivo* model for efficacy studies (i.e., the choice of cisplatin-resistant IGROV-1/Pt1, a cell line where the expression of integrin $\alpha_v\beta_3$ is particularly relevant).

Evaluation of *in vivo* antitumor activity. Antitumor activity of our lead conjugate *cyclo*[DKP- β_3 -RGD]-PTX **11**, delivered i.v. and administered every 4 days for 4 times (q4dx4), was examined on the $\alpha_v\beta_3$ -rich IGROV-1/Pt1 carcinoma grown in athymic mice as subcutaneous (s.c.) tumor. A significant, dose-related antitumor effect was observed following administration of two dose levels of compound **11** (15 mg/kg and 30 mg/kg). Moreover, when

1
2
3
4
5
6
7
8
9
10
11
12
13
14
15
16
17
18
19
20
21
22
23
24
25
26
27
28
29
30
31
32
33
34
35
36
37
38
39
40
41
42
43
44
45
46
47
48
49
50
51
52
53
54
55
56
57
58
59
60

compound **11** (30 mg/kg, i.e. 19.1 $\mu\text{mol/kg}$) was compared to Paclitaxel (30 mg/kg, i.e. 35.1 $\mu\text{mol/kg}$) administered with the same weight dosage and schedule, it displayed better effects in terms of tumor volume inhibition (TVI, 85 vs 76%), despite the lower (ca. half) molar dosage used (Figure 8). Furthermore, 2 out of 8 tumors in animals receiving conjugate **11** disappeared without any evidence of disease until the end of the experiment. Thus, an improved and more persistent effect against the growth of treated tumors was achieved, as indicated also by the higher Log_{10} Cell Kill value (LCK, 1.4 vs 0.7, Table 4). Treatment was well tolerated, as no deaths or significant weight losses were observed among the treated animals.³⁶

Figure 8. *In vivo* antitumor activity studies of *cyclo*[DKP- β -RGD]-PTX **11** compared to Paclitaxel on IGROV-1/Pt1 ovarian carcinoma^a



^aEfficacy of compound **11** (CPD11) and Paclitaxel (PTX) administered intravenously every fourth day for four times on the ovarian carcinoma IGROV-1/Pt1 xenografted subcutaneously in athymic nude mice. The solvent was injected for the control group (\circ). Each point represents the mean tumor volume from 8 tumors. Bars represent S.D. *, $P < 0.05$ by Student's t test on tumor volumes over control mice.

Table 4. *In vivo* antitumor activity and toxicity profile of *cyclo*[DKP- β -RGD]-PTX **11** and Paclitaxel against human ovarian cancer xenografts (IGROV-1/Pt1) in mice, as a function of dose.

Treatment	Dose (mg/kg)	Dose (μ mol/kg)	TVI% ^a	CR ^b	NED ^c	LCK ^d	BWL% ^e	D/T ^f
Paclitaxel	30	35.1	76	3/8	0/8	0.7	4	0/4
<i>Cyclo</i> [DKP- β -RGD]-PTX 11	15	9.6	64	0/8	-	0.3	0	0/4
<i>Cyclo</i> [DKP- β -RGD]-PTX 11	30	19.1	85	2/8	2/8	1.4	3	0/4

^aTVI%: Tumor Volume Inhibition percent in treated over control mice, calculated 10 d after the end of treatments.

^bCR: Complete Response: disappearance of tumors lasting at least 10 days.

^cNED: No Evidence of Disease at the end of experiment (at day 66).

^dLCK: Gross Log₁₀ Cell Kill to reach 600 mm³ of tumor volume (see Figure 8).

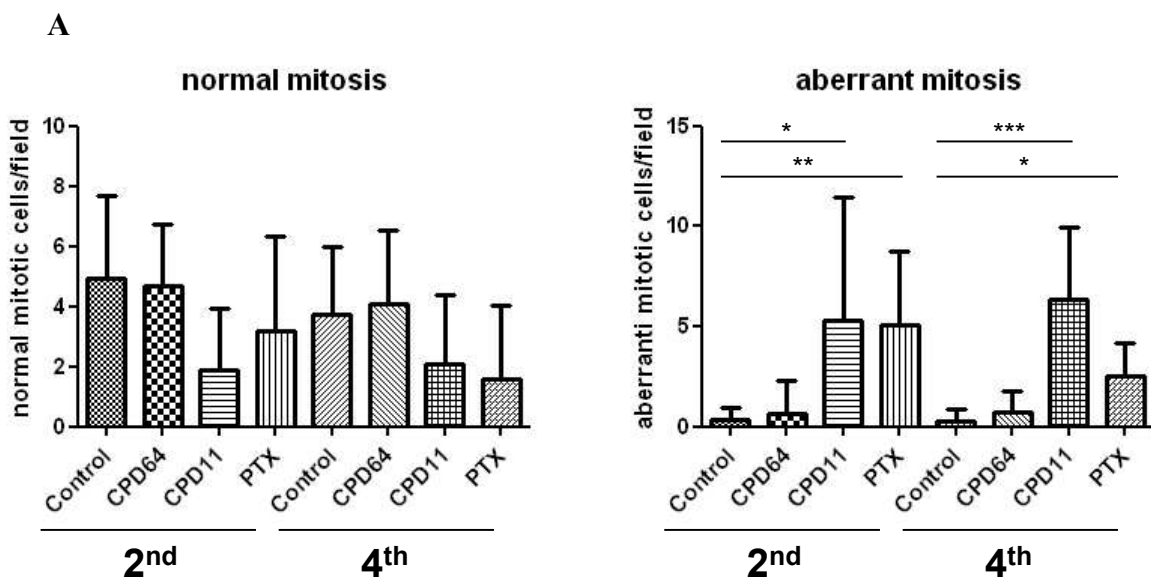
^eBWL%: Body Weight Loss percentage induced by drug treatment.

^fD/T: Dead/Treated mice.

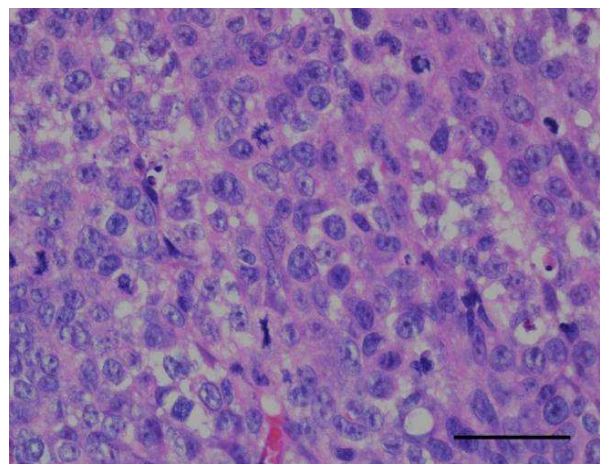
Immunohistochemistry analysis of treatment effects. To investigate the mechanism underlying the improved antitumor activity of *cyclo*[DKP- β -RGD]-PTX **11** over paclitaxel, histopathological analysis was carried out in tumors from untreated mice and from mice treated with *cyclo*[DKP- β -RGD]-PTX **11**, compound **64**, and Paclitaxel (Figure 9). The comparison between Paclitaxel and *cyclo*[DKP- β -RGD]-PTX **11** was carried out administering 30 mg/kg for both compounds, amounts which correspond to 35.1 μ mol/kg for Paclitaxel and to 19.1 μ mol/kg for *cyclo*[DKP- β -RGD]-PTX **11**. Histological analysis indicated the presence of a high number of mitotic cells in the group treated with *cyclo*[DKP- β -RGD]-PTX **11**, compared to the other groups (Figure 9). In addition, the majority of the mitoses observed in the groups treated with

either *cyclo*[DKP- β -RGD]-PTX **11** or Paclitaxel were aberrant, an observation consistent with the mechanism of action of spindle poisons.³⁷ High levels of aberrant mitoses were observed with *cyclo*[DKP- β -RGD]-PTX **11**, already 24 h after the second treatment and persisted after the fourth treatment. On the contrary, the amount of aberrant mitotic cells observed after mice treatment with Paclitaxel decreased over time.

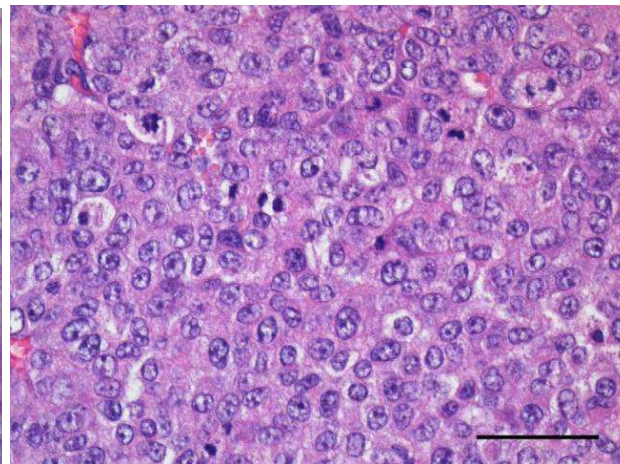
Figure 9. Histopathological analysis of IGROV-1/Pt1 xenograft, after treatment with *cyclo*[DKP- β -RGD]-PTX **11**^a

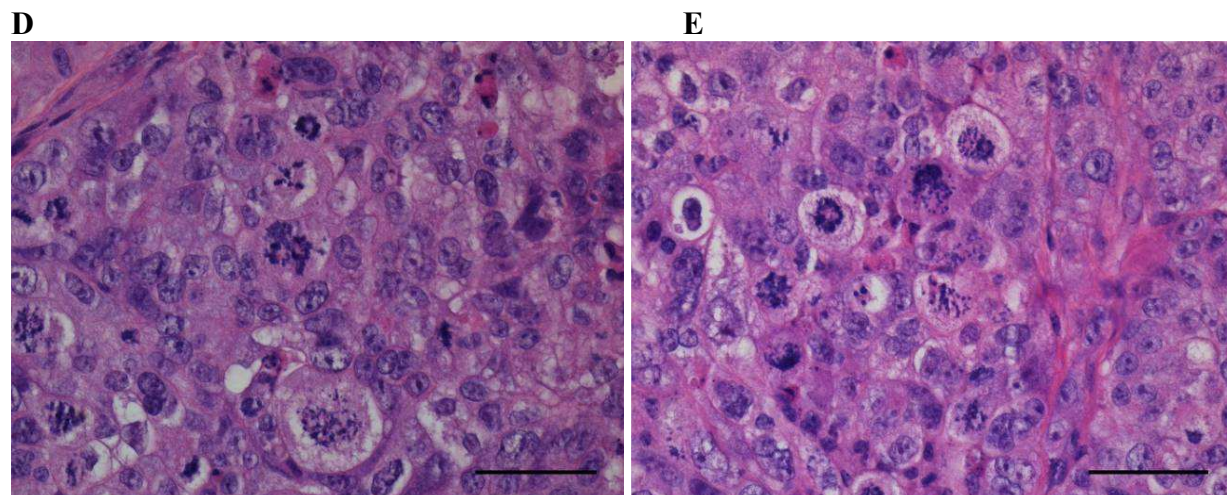


B



C





1
2
3
4
5
6
7
8
9
10
11
12
13
14
15
16
17
18
19
20
21
22
23
24
25
26
27
28
29
30
31
32
33
34
35
36
37
38
39
40
41
42
43
44
45
46
47
48
49
50
51
52
53
54
55
56
57
58
59
60

D **E**

A. Quantitative analysis of mitoses. Mitoses were evaluated in 3 randomly selected 400x fields using quadruplicate samples. The reported numbers correspond to the mean number of normal/aberrant mitoses in analyzed groups: control groups (control); groups treated with compound **64** (CPD64); group treated with compound **11** (CPD11); groups treated with Paclitaxel (PTX). Note that tumors were obtained from mice sacrificed 24 h after the second or the fourth treatment. **B.** Randomly selected high power field (hpf) within the bulk of the tumor from a control group sample, characterized by normal mitoses (hematoxylin and eosin; Bar, 50 μ m). **C.** Randomly selected hpf within the bulk of the tumor from a sample treated with compound **64**. Hyperchromatic nuclei with condensed chromatin are evident (hematoxylin and eosin; Bar, 50 μ m). **D.** Randomly selected hpf within the bulk of the tumor from a sample treated with compound **11**. Note markedly aberrant mitoses, with formation of nuclear envelopes around individual clusters of missegregated chromosomes (mitotic catastrophe) (hematoxylin and eosin; Bar, 50 μ m). **E.** Randomly selected hpf within the bulk of the tumor from a sample treated with Paclitaxel. Note markedly aberrant mitoses, with formation of nuclear envelopes around individual clusters of missegregated chromosomes (mitotic catastrophe) (hematoxylin and eosin; Bar, 50 μ m).

Since tumors from mice treated with *cyclo*[DKP- β -RGD]-PTX **11** had the highest number of mitoses and the major part of them were atypical, it is likely that tumor cells treated with compound **11** entered mitosis, but failed to replicate and incurred in mitotic arrest.

CONCLUSIONS

In conclusion, since α_v integrins are overexpressed on the surface of cancer cells, we have synthesized a small library of integrin ligand - Paclitaxel conjugates **10-13** with the aim of using the tumor-homing *cyclo*[DKP-RGD] peptidomimetics for site-directed delivery of the cytotoxic

1
2
3 drug. All the Paclitaxel-RGD constructs **10-13** inhibited biotinylated vitronectin binding to the
4
5 purified $\alpha_v\beta_3$ receptor at low nanomolar concentration, showing that the enormous increase of
6
7 steric hindrance in the conjugates, due to presence of the linker bearing Paclitaxel through the
8
9 succinate tether, did not influence the high affinity for the integrin receptors. *Cyclo*[DKP-RGD]-
10
11 PTX conjugates **10-13** showed *in vitro* cytotoxic activity against a panel of human tumor cell
12
13 lines similar to that of Paclitaxel. Among the cell lines, the cisplatin-resistant IGROV-1/Pt1 cells
14
15 expressed high levels of integrin $\alpha_v\beta_3$, making them attractive to be tested in *in vivo* models.
16
17 *Cyclo*[DKP-*f*3-RGD]-PTX **11** displayed sufficient stability in physiological solution and in both
18
19 human and murine plasma to be a good candidate for *in vivo* testing. In tumor-targeting
20
21 experiments against the IGROV-1/Pt1 human ovarian carcinoma xenotransplanted in nude mice,
22
23 compound **11** exhibited better effects than Paclitaxel in terms of tumor volume inhibition and
24
25 Log_{10} Cell Kill, despite the lower (ca. half) molar dosage used. Moreover, 2 out of 8 tumors in
26
27 animals receiving conjugate **11** disappeared without any evidence of disease until the end of
28
29 experiment, suggesting an improved and more persistent antitumor effect. Treatment was well
30
31 tolerated, as no deaths or significant weight losses were observed among the treated animals.
32
33 Comparison of the *in vitro* data shown in Table 2 (where conjugate **11** is apparently two-fold less
34
35 cytotoxic than Paclitaxel with respect to the IGROV-1/Pt-1 cancer cell line) with the *in vivo* data
36
37 of Table 4 and Figure 8 (where conjugate **11** shows a superior antitumor effect compared to
38
39 Paclitaxel against the IGROV-1/Pt1 human ovarian carcinoma xenotransplanted in nude mice) is
40
41 not contradictory but rather reinforces the tumor homing effect claimed for compound **11**. In
42
43 fact, *in vivo* the conjugate is targeted to the tumor, whereas *in vitro* it acts through release of
44
45 Paclitaxel. The histological examination of tumor specimens supports this view, because the
46
47 induction of aberrant mitosis observed after treatment with conjugate **11** was more frequent,
48
49
50
51
52
53
54
55
56
57
58
59
60

1
2
3 pronounced and persistent than that observed with Paclitaxel (see Figure 9A, right diagram),
4
5 consistent with a successful drug delivery to the target. The superior *in vivo* activity of
6
7 *cyclo*[DKP- β -RGD]-PTX **11** as compared to Paclitaxel supports the view that integrin ligands
8
9 are promising tools to improve delivery of cytotoxic drugs.
10
11

12 13 14 15 **EXPERIMENTAL SECTION**

16
17
18
19
20 **MATERIALS AND METHODS.** All manipulations requiring anhydrous conditions were
21
22 carried out in flame-dried glassware, with magnetic stirring and under a nitrogen atmosphere. All
23
24 commercially available reagents were used as received. Anhydrous solvents were purchased
25
26 from commercial sources and withdrawn from the container by syringe, under a slight positive
27
28 pressure of nitrogen. (*S*)- and (*R*)-serine methyl ester hydrochloride,³⁸ (*2R*)- and (*2S*)-aspartic
29
30 acid β -allyl ester hydrochloride,³⁹ *N*-(*tert*-butoxycarbonyl)-(*2R*)-aspartic acid β -allyl ester,³⁹ (*S*)-
31
32 and (*R*)-*N*-Boc-serine methyl ester,⁴⁰ (*S*)- and (*R*)-methyl 3-azido-2-(*tert*-
33
34 butoxycarbonylamino)propanoate,⁴¹ (*S*)- and (*R*)-3-azido-2-(*tert*-butoxycarbonylamino)
35
36 propanoic acid,⁴¹ (*S*)- and (*R*)-dimethyl aspartate hydrochloride,⁴² (*S*)- and (*R*)-*N*-benzyl-
37
38 dimethyl aspartate⁴³ and *N*-Boc-glycine benzyl ester⁴⁴ were prepared according to literature
39
40 procedures and their analytical data were in agreement with those already published. Reactions
41
42 were monitored by analytical thin layer chromatography using 0.25 mm pre-coated silica gel
43
44 glass plates (DURASIL-25 UV254) and compounds visualized using UV fluorescence, aqueous
45
46 potassium permanganate or ninhydrin. Flash column chromatography was performed according
47
48 to the method of Still and co-workers⁴⁵ using Chromagel 60 ACC (40-63 μ m) silica gel. Melting
49
50 points were obtained in an open capillary apparatus and are uncorrected. ¹H-NMR spectra were
51
52
53
54
55
56
57
58
59
60

1
2
3 recorded on a spectrometer operating at 400.16 MHz. Proton chemical shifts are reported in ppm
4
5 (δ) with the solvent reference relative to tetramethylsilane (TMS) employed as the internal
6
7 standard. The following abbreviations are used to describe spin multiplicity: s = singlet, d =
8
9 doublet, t = triplet, q = quartet, m = multiplet, br = broad signal, dd = doublet of doublet.
10
11 ^{13}C -NMR spectra were recorded on a spectrometer operating at 100.63 MHz, with complete
12
13 proton decoupling. Carbon chemical shifts are reported in ppm (δ) relative to TMS with the
14
15 respective solvent resonance as the internal standard. Infrared spectra were recorded on a
16
17 standard FT-IR and peaks are reported in cm^{-1} . Optical rotation values were measured on an
18
19 automatic polarimeter with a 1 dm cell at the sodium D line and are given in units of 10^{-1} deg
20
21 $\text{cm}^2 \text{g}^{-1}$. High resolution mass spectra (HRMS) were performed on a Fourier Transform Ion
22
23 Cyclotron Resonance (FT-ICR) Mass Spectrometer APEX II & Xmass software (Bruker
24
25 Daltonics) – 4.7 T Magnet (MagneX) equipped with ESI source, available at CIGA (Centro
26
27 Interdipartimentale Grandi Apparecchiature) c/o Università degli Studi di Milano. Low
28
29 resolution mass spectra (MS) were measured on a Waters Acquity UPLC-MS (ESI ion source).
30
31 All described compounds showed a purity > 98%, as determined by HPLC (UV and MS
32
33 detectors). LC-UV/MS data were collected with an Agilent 1100 HPLC connected to a Bruker
34
35 Esquire 3000+ ion trap mass spectrometer through an ES interface.
36
37
38
39
40
41
42

43 Cancer cell lines IGROV-1 e IGROV-1/Pt1 were obtained as previously reported.⁴⁶ Cancer
44
45 cell lines U2OS, SKOV3, PANC-1 and MIA Paca2 are ATCC cultures, registered as follows.
46
47 U2OS: ATCC HTB-96. SKOV3: ATCC HTB-77. PANC-1: ATCC CRL-1469. MIA PaCa2:
48
49 ATCC CRL-1420.
50
51
52
53
54
55
56
57
58
59
60

1
2
3 **SOLID-PHASE RECEPTOR-BINDING ASSAY.** Purified $\alpha_v\beta_3$ and $\alpha_v\beta_5$ receptors
4
5 (Chemicon International, Inc., Temecula, CA, USA) were diluted to 0.5 $\mu\text{g}/\text{mL}$ in coating buffer
6
7 containing 20 mM Tris-HCl (pH 7.4), 150 mM NaCl, 1 mM MnCl_2 , 2 mM CaCl_2 and 1 mM
8
9 MgCl_2 . An aliquot of diluted receptors (100 $\mu\text{L}/\text{well}$) was added to 96-well microtiter plates
10
11 (NUNC MW 96F MEDISORP STRAIGHT) and incubated overnight at 4 °C. The plates were
12
13 then incubated with blocking solution (coating buffer plus 1% bovine serum albumin) for
14
15 additional 2 hours at room temperature to block nonspecific binding followed by 3-hour
16
17 incubation at room temperature with various concentrations (10^{-12} – 10^{-5} M) of test compounds in
18
19 the presence of 1 $\mu\text{g}/\text{mL}$ biotinylated vitronectine. Biotinylation was performed using EZ-Link
20
21 Sulfo-NHS-Biotinylation kit (Pierce, Rockford, IL). After washing, the plates were incubated for
22
23 1 hour at room temperature with streptavidin-biotinylated peroxidase complex (Amersham
24
25 Biosciences, Uppsala, Sweden) followed by 30 minutes incubation with 100 μL Substrate
26
27 Reagent Solution (R&D Systems, Minneapolis, MN) before stopping the reaction by addition of
28
29 50 μL of 2 N H_2SO_4 . Absorbance at 415 nm was read in a Synergy™ HT Multi-Detection
30
31 Microplate Reader (BioTek Instruments, Inc.). Each data point is the result of the average of
32
33 triplicate wells and was analyzed by nonlinear regression analysis with Prism GraphPad
34
35 program.
36
37
38
39
40
41
42
43
44
45

46 **GENERAL PROCEDURE A FOR DEPROTECTION REACTIONS.** To a solution of the
47
48 *N*-Boc-protected amino acid or peptide in CH_2Cl_2 (0.13 M) was added half volume of TFA and
49
50 the reaction was stirred at rt for 2 h. The solvent was evaporated, toluene (2 \times) was added
51
52 followed by evaporation, and then ether was added and evaporated to afford the corresponding
53
54 TFA salt.
55
56
57
58
59
60

1
2
3
4
5
6 **GENERAL PROCEDURE B FOR COUPLING REACTIONS.** To a solution of the *N*-
7
8 protected amino acid in DMF, under nitrogen atmosphere and at 0 °C, HATU (1.2 equiv), HOAt
9
10 (1.2 equiv) and *i*-Pr₂NEt (4 equiv) were added. After 30 min, a solution of the TFA salt of the
11
12 peptide in DMF was added and the reaction mixture was stirred at 0 °C for 1 h and at rt
13
14 overnight. The mixture was diluted with AcOEt and consecutively washed with 1 M KHSO₄
15
16 (2×), aqueous NaHCO₃ (2×) and brine (2×), dried over Na₂SO₄ and the solvent evaporated under
17
18 reduced pressure to afford the crude product.
19
20
21
22
23

24 **GENERAL PROCEDURE C FOR THE SYNTHESIS OF *cyclo*[DKP-RGD]**
25 **PACLITAXEL CONJUGATES 10-13.** Diisopropylcarbodiimide (11.93 μL, 9.72 mg, 0.077
26
27 mmol, 1.9 equiv) was added to a solution of 2'-succinyl-Paclitaxel **67** (49 mg, 0.0513 mmol,
28
29 1.25 equiv) and *N*-hydroxysulfosuccinimide sodium salt (13.94 mg, 0.0642 mmol, 1.55 equiv) in
30
31 dry dimethylformamide (2.0 mL). The resulting solution was stirred under argon at room
32
33 temperature for 24 h. Volatiles were then removed *in vacuo* to give an off-white solid, which was
34
35 re-dissolved in acetonitrile (2 mL). A solution of the appropriate *cyclo*[DKP-RGD] (**63-66**) (35
36
37 mg, 0.0414 mmol) in pH 7.0 phosphate buffer (0.5 M, 1.0 mL) was then added to the acetonitrile
38
39 solution, and the pH was adjusted to 7.3 with NaOH (0.2 M, a few drops). The resulting solution
40
41 was rapidly cooled to 0 °C and stirred for 10 hours, warmed to room temperature and stirred for
42
43 further 18 h. During the entire period the pH value was kept near 7.3 adding 0.1 M aqueous
44
45 NaOH, when required. Dioxane/water (1:1, 10 mL) was then added to the reaction mixture and
46
47 the resulting solution was freeze-dried. The solid recovered from freeze-drying was purified by
48
49 semipreparative-HPLC [Water's Atlantis 21 mm x 10 cm column, gradient: 90% (H₂O + 0.1%
50
51
52
53
54
55
56
57
58
59
60

HCOOH) / 10% (CH₃CN + 0.1% HCOOH) to 30% (H₂O + 0.1% HCOOH) / 70% (CH₃CN + 0.1% HCOOH)]. The purified products were then freeze dried to give the desired compounds (**10-13**) as white solids.

Cyclo[DKP-f2-RGD]-PTX 10. Compound **10** was synthesized according to general procedure C (40 mg, 60% yield). ¹H NMR (400 MHz, CD₃OD) δ 8.09 (dd, 2H, $J = 8.4, 1.2$ Hz), 7.84 (dd, 2H, $J = 7.1, 1.6$ Hz), 7.74 (tt, 1H, $J = 6.8, 1.6$ Hz), 7.64 (t, 2H, $J = 7.6$ Hz), 7.59-7.54 (m, 1H), 7.49-7.44 (m, 6H), 7.28-7.25 (m, 4H), 7.22 (tt, 1H, $J = 5.8, 2.8$ Hz), 6.43 (s, 1H), 5.98 (t, 1H, $J = 9.1$ Hz), 5.69 (d, 1H, $J = 7.9$ Hz), 5.61 (d, 1H, $J = 7.0$ Hz), 5.45 (d, 1H, $J = 7.9$ Hz), 5.24 (d, 1H, $J = 15.1$ Hz), 5.10 (dd, 1H, $J = 9.7, 1.6$ Hz), 4.77 (m overlapped with water signal, 1H), 4.65 (m overlapped with water signal, 1H), 4.40-4.30 (m, 4H), 4.21 (m, 3H), 4.08 (d, 2H, $J = 15.7$ Hz), 3.85 (d, 1H, $J = 4.6$ Hz), 3.78 (d, 1H, $J = 7.0$ Hz), 3.64 (d, 1H, $J = 16.3$ Hz), 3.28 (m overlapped with solvent signal, 1H), 3.22 (t, 2H, $J = 6.7$ Hz), 2.98 (dd, 1H, $J = 13.2, 7.4$ Hz), 2.84-2.75 (m, 2H), 2.71-2.68 (m, 2H), 2.64-2.50 (m, 3H), 2.37-2.34 (m, 4H), 2.18 (s, 3H), 2.01 (m, 1H), 1.89-1.79 (m, 5H), 1.75-1.59 (m, 7H), 1.14 (s, 3H), 1.11 (s, 3H); ¹³C NMR (101 MHz, CD₃OD) δ 205.7, 175.8, 175.0, 174.5, 174.17, 174.02, 173.7, 172.09, 171.96, 171.1, 170.74, 170.54, 169.8, 168.0, 158.3, 142.3, 139.6, 137.9, 135.5, 135.04, 134.95, 134.7, 133.2, 131.1, 130.8, 130.2, 129.94, 129.82, 129.71, 129.3, 129.0, 128.64, 128.46, 85.9, 82.0, 79.1, 77.5, 76.7, 76.14, 76.06, 72.9, 72.1, 60.3, 59.1, 55.8, 55.4, 53.2, 51.3, 48.1, 47.8, 44.3, 43.7, 43.0, 40.7, 39.9, 37.32, 37.21, 36.0, 31.0, 29.9, 28.2, 26.8, 26.2, 23.4, 22.3, 20.9, 15.0, 10.6; IR (film) 3361, 3075, 2940, 1730, 1715, 1698, 1667, 1538, 1422, 1243, 1135, 1072 cm⁻¹; MS (ESI) m/z calcd. for [C₇₈H₉₂N₁₁O₂₄]⁺: 1566.63 [M+H]⁺; found: 1566.6.

Cyclo[DKP-*f3*-RGD]-PTX 11. Compound **11** was synthesized according to general procedure C (47 mg, 70% yield). ¹H NMR (400 MHz, CD₃OD) δ 8.12 (dd, 2H, *J* = 8.5, 1.4 Hz), 7.83 (dd, 2H, *J* = 8.5, 1.4 Hz), 7.71-7.66 (m, 1H), 7.60 (t, 2H, *J* = 7.5 Hz), 7.56-7.52 (m, 1H), 7.50-7.42 (m, 6H), 7.30 (s, 4H), 7.25 (tt, 1H, *J* = 7.1, 1.6 Hz), 6.45 (s, 1H), 6.05 (td, 1H, *J* = 9.1, 1.0 Hz), 5.79 (d, 1H, *J* = 6.5 Hz), 5.64 (d, 1H, *J* = 7.2 Hz), 5.44 (d, 1H, *J* = 6.5 Hz), 5.13 (d, 1H, *J* = 14.9 Hz), 5.03 (dd, 1H, *J* = 9.4, 1.6 Hz), 4.91-3.86 (m, 1H), 4.75 (dd, 1H, *J* = 6.5, 4.7 Hz), 4.44-4.36 (m, 3H), 4.30-4.22 (m, 2H), 4.20 (br s, 2H, *J* = 4.2 Hz), 4.16 (ddd, 1H, *J* = 12.0, 8.7, 3.6 Hz), 4.09-4.08 (m, 2H), 3.90 (d, 1H, *J* = 6.0 Hz), 3.82 (d, 1H, *J* = 7.1 Hz), 3.74-3.68 (m, 2H), 3.61 (d, 1H, *J* = 17.2 Hz), 3.54 (dt, 1H, *J* = 11.7, 2.8 Hz), 3.42 (dd, 1H, *J* = 14.6, 6.4), 3.27-3.16 (m, 2H), 2.80-2.75 (m, 2H), 2.72-2.51 (m, 7H), 2.37 (s, 3H), 2.18-2.12 (m, 4H), 2.09-2.01 (m, 1H), 1.92 (s, 3H), 1.86-1.76 (m, 3H), 1.68-1.63 (m, 5H), 1.14 (s, 3H), 1.13 (s, 3H); ¹³C NMR (101 MHz, CD₃OD) δ 205.5, 174.0, 173.60, 173.46, 173.0, 171.63, 171.54, 171.46, 171.2, 170.5, 167.7, 142.4, 140.2, 138.4, 135.5, 134.80, 134.63, 132.9, 131.39, 131.22, 130.1, 129.72, 129.60, 129.56, 129.3, 128.6, 100.0, 85.9, 82.3, 79.0, 77.5, 76.9, 76.2, 75.9, 72.9, 72.4, 61.6, 60.6, 59.2, 55.4, 54.4, 53.2, 50.5, 48.0, 44.6, 43.76, 43.69, 42.2, 39.9, 37.6, 36.49, 36.36, 31.1, 29.8, 27.7, 26.9, 26.5, 25.1, 23.3, 22.3, 20.8, 15.1, 10.5; IR (film) 3360, 3075, 2940, 1729, 1714, 1693, 1665, 1537, 1421, 1241, 1135, 1071 cm⁻¹; MS (ESI) *m/z* calcd. for [C₇₈H₉₂N₁₁O₂₄]⁺: 1566.63 [M+H]⁺; found: 1566.6.

Cyclo[DKP-*f4*-RGD]-PTX 12. Compound **12** was synthesized according to general procedure C (42 mg, 63% yield). ¹H NMR (400 MHz, DMSO-*d*₆) δ 9.22 (d, 1H, *J* = 8.5 Hz), 8.95 (s, 1H), 8.79 (s, 1H), 8.44-8.40 (m, 1H), 8.35 (t, 1H, *J* = 5.7 Hz), 8.20 (s, 1H), 7.98 (dd, 2H, *J* = 7.1, 1.3 Hz), 7.86 (dd, 2H, *J* = 7.2, 1.3 Hz), 7.76-7.69 (m, 1H, *J* = 1.5 Hz), 7.69-7.63 (m, 2H), 7.59-7.53

1
2
3 (m, 1H), 7.49 (d, 1H, $J = 7.6$ Hz), 7.46-7.42 (m, 5H), 7.23-7.17 (m, 5H), 6.30 (s, 1H), 5.83 (t,
4
5 1H, $J = 8.9$ Hz), 5.54 (t, 1H, $J = 8.7$ Hz), 5.42 (d, 1H, $J = 7.1$ Hz), 5.36 (d, 1H, $J = 8.9$ Hz), 5.21
6
7 (d, 1H, $J = 14.4$ Hz), 4.92 (d, 2H, $J = 10.6$ Hz), 4.62 (s, 1H), 4.27-4.07 (m, 5H), 4.04-3.99 (m,
8
9 3H), 3.94-3.87 (m, 1H), 3.83-3.79 (m, 1H), 3.70 (br s, 2H), 3.58 (d, 1H, $J = 7.1$ Hz), 3.43-3.26
10
11 (m overlapped with water signal, 2H), 3.07 (br s, 2H), 2.89 (br s, 2H), 2.69-2.56 (m, 3H), 2.45 (t,
12
13 2H, $J = 6.8$ Hz), 2.38-2.30 (m, 2H), 2.24-2.20 (m, 4H), 2.10 (s, 3H), 1.84-1.76 (m, 5H), 1.64 (t,
14
15 1H, $J = 12.4$ Hz), 1.54-1.41 (m, 7H), 1.02 (s, 3H), 1.00 (s, 3H); ^{13}C NMR (101 MHz, DMSO- d_6)
16
17 δ 202.3, 173.9, 172.13, 171.94, 170.8, 170.2, 169.63, 169.50, 169.1, 168.84, 168.74, 168.3,
18
19 167.9, 166.4, 165.2, 157.3, 139.4, 138.7, 137.3, 134.8, 134.3, 133.45, 133.33, 132.7, 131.4,
20
21 129.95, 129.93, 129.56, 129.54, 128.73, 128.65, 128.55, 128.29, 128.14, 127.83, 127.71, 127.65,
22
23 127.4, 83.6, 80.2, 76.7, 75.3, 74.68, 74.54, 74.50, 72.5, 70.7, 70.4, 57.4, 56.1, 53.98, 53.86,
24
25 52.17, 52.13, 46.1, 44.9, 42.9, 42.1, 41.9, 40.1, 39.9, 38.2, 36.5, 35.7, 34.4, 29.5, 28.7, 27.6, 26.3,
26
27 25.3, 22.5, 21.4, 20.63, 20.52, 13.9, 9.7; IR (film) 3370, 3071, 2941, 1731, 1714, 1699, 1667,
28
29 1538, 1421, 1243, 1135, 1071 cm^{-1} ; MS (ESI) m/z calcd. for $[\text{C}_{78}\text{H}_{92}\text{N}_{11}\text{O}_{24}]^+$: 1566.63 $[\text{M}+\text{H}]^+$;
30
31 found: 1566.6
32
33
34
35
36
37
38
39
40

41 **Cyclo[DKP-f6-RGD]-PTX 13.** Compound **13** was synthesized according to general procedure
42
43 C (43 mg, 65% yield). ^1H NMR (400 MHz, DMSO- d_6) δ 9.42 (s, 1H), 9.25 (d, 1H, $J = 8.5$ Hz),
44
45 8.74 (s, 1H), 8.62 (s, 1H), 8.45 (s, 1H), 8.37 (t, 1H, $J = 5.7$ Hz), 7.99-7.97 (m, 2H), 7.87-7.84 (m,
46
47 3H), 7.73 (t, 1H, $J = 7.3$ Hz), 7.66 (t, 2H, $J = 7.4$ Hz), 7.56 (tt, 1H, $J = 7.3, 2.0$ Hz), 7.50-7.44
48
49 (m, 7H), 7.25-7.15 (m, 5H), 6.30 (s, 1H), 5.83 (t, 1H, $J = 8.8$ Hz), 5.53 (t, 1H, $J = 8.7$ Hz), 5.41
50
51 (d, 1H, $J = 7.2$ Hz), 5.35 (d, 1H, $J = 9.0$ Hz), 5.11 (d, 1H, $J = 14.9$ Hz), 4.98-4.90 (t, 2H), 4.64 (s,
52
53 1H), 4.29-4.20 (m, 3H), 4.17-4.08 (m, 2H), 4.04-3.95 (m, 3H), 3.93-3.79 (m, 3H), 3.74-3.64 (m,
54
55
56
57
58
59
60

1
2
3 1H), 3.59 (d, 1H, $J = 6.8$ Hz), 3.53-3.43 (m, 1H), 3.26-3.19 (m, 1H), 3.07 (br s, 1H), 2.97 (br s,
4
5 1H), 2.72-2.58 (m, 4H), 2.56-2.52 (m, 1H), 2.45 (t, 2H, $J = 6.8$ Hz), 2.40-2.28 (m, 2H), 2.23 (s,
6
7 3H), 2.10 (s, 3H), 1.82-1.60 (m, 7H), 1.52-1.46 (m, 6H), 1.02 (s, 3H), 1.00 (s, 3H); ^{13}C NMR
8
9 (101 MHz, $\text{DMSO-}d_6$) δ 202.7, 172.0, 171.8, 170.3, 169.72, 169.57, 169.2, 168.79, 168.72,
10
11 166.8, 166.4, 165.2, 157.3, 139.5, 137.4, 135.2, 134.3, 133.5, 133.32, 133.28, 132.7, 131.5,
12
13 129.9, 129.6, 128.7, 128.38, 128.21, 128.0, 127.7, 127.5, 83.6, 80.3, 76.7, 75.3, 74.69, 74.62,
14
15 74.49, 70.7, 70.4, 57.2, 54.4, 54.1, 51.98, 51.92, 46.10, 45.97, 43.0, 41.9, 40.9, 39.7, 37.8, 36.6,
16
17 34.4, 29.5, 28.7, 28.0, 26.4, 24.4, 22.6, 21.4, 20.7, 14.0, 9.8; IR (film) 3365, 3071, 2940, 1732,
18
19 1716, 1699, 1665, 1537, 1421, 1243, 1135, 1071 cm^{-1} ; MS (ESI) m/z calcd. for $[\text{C}_{78}\text{H}_{92}\text{N}_{11}\text{O}_{24}]^+$:
20
21 1566.63 $[\text{M}+\text{H}]^+$; found: 1566.6.
22
23
24
25
26
27
28
29
30
31

32 **PLASMA STABILITY ASSAYS.** A 10 mM stock solution of *cyclo*[DKP- β -RGD]-PTX **11**
33 (MW 1566.62) was obtained by dissolving 2 mg of compound in 127.66 μL of DMSO. A further
34 dilution 1:50 in pH 7.5 phosphate buffer (PBS) was performed (10 μL of stock solution into 490
35 μL PBS) to obtain a 200 μM solution; from this last solution, 25 μL were spiked into 475 μL of
36 plasma (murine or human) to obtain the final concentration of 10 μM . Standards (lidocaine and
37 2-Piperidinoethyl-4-amino-5-chloro-2-methoxybenzoate) were tested at 2.5 μM final
38 concentration starting from a 500 μM stock solution in DMSO, further diluted 1:10 into PBS and
39 1:20 into plasma.
40
41
42
43
44
45
46
47
48
49
50

51 Aliquots of 50 μL volume were taken at 0, 15, 30, 60, 120, 180 and 300 minutes of incubation
52 at 37 $^\circ\text{C}$ and immediately quenched with 200 μL of a solution of Verapamil 250 ng/mL (internal
53 standard) in acetonitrile. Samples were centrifuged for 20 min at 3000 rpm and supernatants
54
55
56
57
58
59
60

1
2
3 analyzed by UPLC (Waters) interfaced with a Premiere XE Triple Quadrupole (Waters). Eluents
4 were Phase A: 95% H₂O, 5% CH₃CN + 0.1% HCOOH and Phase B: 5% H₂O, 95% CH₃CN +
5
6 0.1% HCOOH. Waters UPLC: flow 0.6 mL/min, column BEH C18, 50x2.1 mm 1.7 μm at 50 °C,
7
8 vol inj. 5 μL. Samples were analyzed in multiple reaction monitoring (MRM) conditions: ESI
9
10 Positive, Desolvation Temperature 450 °C, Desolvation Gas 900 L/h, Cone Gas 90 L/h, Collision
11
12 Gas 0.2 L/h. Results are presented as Mean ± S.D., n=2 for standards, n=3 for *cyclo*[DKP-β-
13
14 RGD]-PTX 11.
15
16
17
18
19
20
21

22 **CELL SENSITIVITY STUDIES.** The human ovarian carcinoma IGROV-1 cell line,⁴⁶ the
23 cisplatin-resistant IGROV-1/Pt1 subline⁴⁶ the human ovarian carcinoma cell line SKOV3, the
24 human pancreatic carcinoma cell lines PANC-1 and MIA-PaCa2 were cultured in Dulbecco's
25 Modified Eagle Medium (DMEM) medium; the human osteosarcoma U2-OS cell line was grown
26 in Mc Coy's 5A medium; HDFC cells were cultured in DMEM-F12 medium. In all cases, the
27 medium was supplemented with 10% fetal calf serum. The cell sensitivity to drugs was measured
28 by using the growth-inhibition assay based on cell counting. Cells were seeded in duplicates into
29 6-well plates and exposed to drug 24 h later. Paclitaxel and the studied compounds were
30 dissolved in DMSO and then added to culture medium. DMSO concentration in medium never
31 exceeded 0.25%. After 72 h of drug incubation, cells were harvested for counting with a cell
32 counter (Z1 Beckman Coulter counter). IC₅₀ is defined as the drug concentration producing 50%
33 decrease of cell growth. At least five independent experiments were performed.
34
35
36
37
38
39
40
41
42
43
44
45
46
47
48
49
50
51
52

53 **ANALYSIS OF INTEGRIN LEVELS.** The expression of integrins was measured by flow
54 cytometry, following optimization of antibody concentration. Exponentially growing cells were
55
56
57
58
59
60

1
2
3 harvested and incubated for 30 min at 4 °C with anti human $\alpha_v\beta_3$ or $\alpha_v\beta_5$ antibodies or isotypic
4 controls (Millipore, Temecula, CA; Chemicon International). Cells were then washed and
5
6 samples were immediately used for flow cytometric analysis (FACScan, Becton-Dickinson).
7
8
9
10 Expression of integrins was expressed as ratio between the mean fluorescence intensity obtained
11
12 in cells incubated with anti-integrin antibodies divided by that of cells incubated with isotypic
13
14 control.
15
16
17
18
19

20 ***IN VIVO* ANTITUMOR ACTIVITY STUDIES.** All experiments were carried out using
21
22 female athymic Swiss nude mice, 8-10 weeks-old (Charles River, Calco, Italy). Mice were
23
24 maintained in laminar flow rooms keeping temperature and humidity constant. Mice had free
25
26 access to food and water. Experiments were approved by the Ethics Committee for Animal
27
28 Experimentation of the Istituto Nazionale Tumori of Milan according to institutional guidelines.
29
30 The IGROV-1/Pt1 human tumor xenograft, derived from cultures of the corresponding ovarian
31
32 carcinoma cell line,⁴⁶ was used. Exponentially growing cells (10^7 /mouse) were s.c. injected into
33
34 the right flank of athymic nude mice and the tumor line was achieved by serial s.c. passages of
35
36 fragments of re-growing tumors into healthy mice. Groups of four mice bearing bilateral s.c.
37
38 tumors were employed. Tumor fragments were implanted on day 0 and tumor growth was
39
40 followed by biweekly measurements of tumor diameters with a Vernier caliper. Tumor volume
41
42 (TV) was calculated according to the formula: $TV \text{ (mm}^3\text{)} = d^2 \times D / 2$ where d and D are the
43
44 shortest and the longest diameter, respectively. Compounds were delivered i.v. and administered
45
46 every 4 days for 4 times (q4dx4). Treatment started three days after tumor implant, when tumors
47
48 were just palpable. The efficacy of the drug treatment was assessed as: 1) Tumor volume
49
50 inhibition percentage (TVI%) in treated versus control mice, calculated as: $TVI\% = 100 - (\text{mean}$
51
52
53
54
55
56
57
58
59
60

1
2
3 TV treated/mean TV control x 100); 2) Log₁₀ cell kill (LCK) calculated by the formula: LCK =
4 (T-C)/3.32xDT where T and C are the mean times (days) required for treated (T) and control (C)
5 tumors, respectively, to reach an established TV and DT is the doubling time of control tumors,
6 obtained from semilog best-fit curves of mean tumor volumes plotted against time; 3) Complete
7 regression (CR), i.e. disappearance of the tumor lasting at least 10 days after the end of
8 treatments. Tumors not regrown at the end of experiment were considered no evidence of disease
9 (NED). The toxicity of the drug treatment was determined as body weight loss (BWL) and lethal
10 toxicity (D/T, dead/treated mice). The highest body weight loss percentage induced by
11 treatments is reported in the Tables. Deaths occurring in treated mice before the death of the first
12 control mouse were ascribed to toxic effects. Two-sided Student's t test was used for statistical
13 comparison of tumor volumes in control over treated mice. For *in vivo* studies, Paclitaxel was
14 dissolved in a mixture of ethanol and cremophor ELP (50+50%) and kept at 4 °C. At treatment
15 the drug was diluted in 90% of cold saline after magnetic stirring and administered i.v..
16
17 *Cyclo*[DKP-*f*3-RGD]-PTX **11** was dissolved and administered like Paclitaxel at room
18 temperature.
19
20
21
22
23
24
25
26
27
28
29
30
31
32
33
34
35
36
37
38
39
40

41 **IMMUNOHISTOCHEMISTRY.** Tumor xenografts and adjacent tissues were excised and
42 formalin fixed and paraffin embedded. Four μm sections from each tumor xenograft were
43 routinely stained with Hematoxylin-Eosin (HE) and evaluated under a light microscope. Mitoses
44 were evaluated in 3 randomly selected 400x fields within the bulk of the xenograft, avoiding
45 areas of necrosis and hemorrhage. The total number of mitoses and the mean value for each
46 sample were evaluated. Furthermore, mitoses were classified as “normal” and “aberrant”,
47 considering in this latter class both small condensed hyperchromatic nuclei and large cells
48
49
50
51
52
53
54
55
56
57
58
59
60

1
2
3 composed by nuclear envelope around individual clusters of missegregated chromosomes
4
5 (mitotic catastrophe), and the ratio between these two classes was evaluated. The analysis of
6
7 mitoses was performed in a blind fashion. Statistical analysis of the obtained data was carried out
8
9 with Kruskal Wallis test followed by Dunn's multiple comparison test using GraphPad Prism
10
11 (GraphPad Software, Inc.).
12
13
14
15
16

17 ASSOCIATED CONTENT

19 Supporting Information

20
21 General information for the synthesis, biological procedures, detailed experimental procedures
22
23 for the synthesis of compounds **10-68**. ^1H and ^{13}C -NMR for all new compounds. This material is
24
25 available free of charge via the Internet at <http://pubs.acs.org>.
26
27
28
29
30

31 AUTHOR INFORMATION

33 Corresponding authors

34
35 * For C.G.: phone, +39-02-50314091; fax, +39-02-50314072; e-mail, cesare.gennari@unimi.it.
36
37

38
39 For U.P.: phone, +39-031-2386444; fax, +39-031-2386449; e-mail,
40
41 umberto.piarulli@uninsubria.it.
42
43

44 Notes

45
46 The authors declare no competing financial interest.
47
48
49

50 ACKNOWLEDGEMENTS

51
52 We thank Milan University for PhD Fellowships (to M.M. and R.C.) and Indena S.p.A. for a generous
53
54 gift of Paclitaxel. We also gratefully acknowledge Ministero dell'Università e della Ricerca for financial
55
56
57
58
59
60

1
2
3 support (PRIN project: Synthesis and biomedical applications of tumor-targeting peptidomimetics). U.P.
4
5 thanks Fondazione CARIPLO for a research grant (Project: RedDrug-Train).
6
7
8
9

10 ABBREVIATIONS USED

11
12 DKP, diketopiperazine; Mtr, 4-methoxy-2,3,6-trimethylbenzenesulphonamide; HATU, *O*-(7-
13
14 azabenzotriazol-1-yl)-*N,N,N',N'*-tetramethyluronium hexafluorophosphate; Tol, toluene; TEA,
15
16 triethylamine; HOAT, 1-hydroxy-7-azabenzotriazole; DIAD, diisopropyl azodicarboxylate;
17
18 BOC-ON, 2-(Boc-oxyimino)-2-phenylacetonitrile; DCU, *N,N'*-dicyclohexylurea; PyBrOP,
19
20 bromotripyrrolidinophosphonium hexafluorophosphate; DPPA, diphenyl phosphoryl azide; EDT,
21
22 1,2-ethanedithiol; TIPS, triisopropylsilane; DIC, *N,N'*-diisopropylcarbodiimide; sulfo-NHS, *N*-
23
24 hydroxysulfosuccinimide sodium salt; PTX, Paclitaxel; RP-HPLC, reverse phase high-pressure
25
26 liquid chromatography; HDFC, human dermal fibroblast cells; TVI, tumor volume inhibition;
27
28 CR, complete response; NED, no evidence of disease; LCK, log₁₀ cell kill; BWL, body weight
29
30 loss; D/T, dead/treated mice; CPD, compound; MRM, multiple reaction monitoring; DMEM,
31
32 Dulbecco's modified eagle medium; TV, tumor volume.
33
34
35
36
37
38
39

40 REFERENCES

41
42
43
44 (1) Broxterman, H. J.; Lankelma, J.; Hoekman, K. Resistance to cytotoxic and anti-angiogenic
45
46 anticancer agents: similarities and differences. *Drug Resist. Updates*. **2003**, *6*, 111-127.
47
48

49
50 (2) Siepmann, J.; Siegel, R. A.; Rathbone, M. J. Fundamentals and applications of controlled
51
52 release drug delivery. Springer: New York, **2012**; pp 493-516.
53
54

55
56 (3) (a) Lammers, T.; Kiessling, F.; Hennink W. E.; Storm G. Drug targeting to tumors:
57
58 Principles, pitfalls and (pre-) clinical progress. *J. Controlled Release* **2012**, *161*, 175-187. (b)
59
60

1
2
3
4
5 Kratz, F.; Müller, I. A.; Ryppa C.; Warnecke A. Prodrug Strategies in Anticancer Chemotherapy.
6
7
8 *ChemMedChem*. **2008**, *3*, 20–53.

9
10
11 (4) (a) Low, P. S. The Optimal Strategy for Drug Targeting. *Mol. Pharmacol.* **2007**, *4*, 629-
12
13 630. (b) Aina, O. H.; Liu, R. W.; Sutcliffe J. L.; Marik, J.; Pan, C. X.; Lam, K. S. From
14
15 Combinatorial Chemistry to Cancer-Targeting Peptides. *Mol. Pharmacol.* **2007**, *4*, 631-651.

16
17
18 (5) (a) Ruoslahti, E.; Bhatia, S. N.; Sailor, M. J. Targeting of drugs and nanoparticles to
19
20 tumors. *J. Cell Biol.* **2010**, *188*, 759–768. (b) Mahato, R.; Tai, W.; Cheng, K. Prodrugs for
21
22 improving tumor targetability and efficiency. *Adv. Drug Delivery. Rev.* **2011**, *63*, 659-670.

23
24
25 (6) Lu, X.; Lu, D.; Scully, M.; Kakkar, V. The role of integrins in cancer and the development
26
27 of anti-integrin therapeutic agents for cancer therapy. *Perspect. Med. Chem.* **2008**, *2*, 57-73.

28
29
30 (7) Barczyk, M.; Carracedo, S.; Gullberg D. Integrins. *Cell Tissue Res.* **2010**, *339*, 269–280.

31
32
33 (8) Hynes, R. O. Integrins: bidirectional, allosteric signaling machines. *Cell* **2002**, *110*, 673-
34
35 687.

36
37
38 (9) (a) Shimaoka, M.; Springer, T. A. Therapeutic antagonists and conformational regulation of
39
40 integrin function. *Nature Rev. Drug Discov.* **2003**, *2*, 703-716. (b) Rathinam, R.; Alahari, S. K.
41
42 Important role of integrins in the cancer biology. *Cancer Metastasis Rev.* **2010**, *29*, 223–237.

43
44
45 (10) Plow, E. F.; Haas, T. A.; Zhang, L.; Loftus, J.; Smith, J. W. Ligand Binding to Integrins.
46
47
48
49
50
51 *J. Biol. Chem.* **2000**, *275*, 21785-21788.

(11) Dechantsreiter, M. A.; Planker, E.; Mathä, B.; Lohof, E.; Hölzemann, G.; Jonczyk, A.; Goodman, S. L.; Kessler, H. *N*-Methylated cyclic RGD peptides as highly active and selective $\alpha_v\beta_3$ integrin antagonists. *J. Med. Chem.* **1999**, *42*, 3033-3040.

(12) Gottschalk, K. E.; Kessler, H. The structures of integrins and integrin-ligand complexes: implications for drug design and signal transduction. *Angew. Chem. Int. Ed.* **2002**, *41*, 3967-3774.

(13) Mas-Moruno, C.; Rechenmacher, F.; Kessler, H. Cilengitide: the first anti-angiogenic small molecule drug candidate design, synthesis and clinical evaluation. *Anti-Cancer Agents Med. Chem.* **2010**, *10*, 753-768.

(14) Xiong, J.-P.; Stehle, T.; Zhang, R.; Joachimiak, A.; Frech, M.; Goodman, S. L.; Arnaout, M. A. Crystal structure of the extracellular segment of integrin $\alpha_v\beta_3$ in complex with an Arg-Gly-Asp ligand. *Science* **2002**, *296*, 151-155.

(15) Auzzas, L.; Zanardi, F.; Battistini, L.; Burreddu, P.; Carta, P.; Rassu, G.; Curti, C.; Casiraghi G. Targeting $\alpha_v\beta_3$ integrin: design and applications of mono- and multifunctional RGD-based peptides and semipeptides. *Curr. Med. Chem.* **2010**, *17*, 1255-1299.

(16) (a) Ressurreicao, A. S. M.; Vidu, A.; Civera, M.; Belvisi, L.; Potenza, D.; Manzoni, L.; Ongeri, S.; Gennari, C.; Piarulli, U. Cyclic RGD-Peptidomimetics containing bifunctional diketopiperazine scaffolds as new potent integrin ligands. *Chem.-Eur. J.* **2009**, *15*, 12184-12188.

(b) Marchini, M.; Mingozi, M.; Colombo, R.; Guzzetti, I.; Belvisi, L.; Vasile, F.; Potenza, D.; Piarulli, U.; Arosio, D.; Gennari, C. Cyclic RGD-Peptidomimetics containing bifunctional diketopiperazine scaffolds as new potent integrin ligands. *Chem.-Eur. J.* **2012**, *18*, 6195-6207.

1
2
3
4
5 (17) (a) Reynolds, A. R.; Hart, I. R.; Watson, A. R.; Welti, J. C.; Silva, R. G.; Robinson, S. D.;
6 Da Violante, G.; Gourlaouen, M.; Salih, M.; Jones, M. C.; Jones, D. T.; Saunders, G.; Kostourou,
7 V.; Perron-Sierra, F.; Norman, J. C.; Tucker, G. C.; Hodivala-Dilke K. M. Stimulation of tumor
8 growth and angiogenesis by low concentrations of RGD-mimetic integrin inhibitors. *Nat. Med.*
9 **2009**, *15*, 392-400. (b) Weis, S. M.; Stupack, D. G.; Cheresch, D. A. Agonizing Integrin
10 Antagonists?. *Cancer Cell* **2009**, *15*, 359-361. (c) Shabbir, S.H.; Eisenberg, J.L.; Mrksich, M. An
11 inhibitor of a cell adhesion receptor stimulates cell migration. *Angew. Chem. Int. Ed.* **2010**, *49*,
12 7706-7709. (d) Robinson, S. D.; Hodivala-Dilke, K. M. The role of $\beta 3$ -integrins in tumor
13 angiogenesis: context is everything. *Curr. Opin. Cell Biol.* **2011**, *23*, 630-637.

14
15
16
17
18
19
20
21
22
23
24
25
26
27 (18) Chen, K.; Chen, X. Integrin Targeted Delivery of Chemotherapeutics. *Theranostics* **2011**,
28 *1*, 189-200.

29
30
31
32
33 (19) (a) Arap, W.; Pasqualini, R.; Ruoslahti, E. Cancer treatment by targeted drug delivery to
34 tumor vasculature in a mouse model. *Science* **1998**, *279*, 377-80. (b) Kim, J. W.; Lee, H. S.
35 Tumor targeting by doxorubicin-RGD-4C peptide conjugate in an orthotopic mouse hepatoma
36 model. *Int. J. Mol. Med.* **2004**, *14*, 529-535.

37
38
39
40
41
42
43 (20) Burkhart, D. J.; Kalet, B. T.; Coleman, M. P.; Post, G. C.; Koch, T. H. Doxorubicin-
44 formaldehyde conjugates targeting $\alpha v \beta 3$ integrin. *Mol. Cancer Ther.* **2004**, *3*, 1593-604.

45
46
47
48 (21) Ryppa, C.; Mann-Steinberg, H.; Fichtner, I.; Weber, H.; Satchi-Fainaro, R.; Biniossek,
49 M.L.; Kratz, F. In vitro and in vivo evaluation of doxorubicin conjugates with the divalent
50 peptide E-[c(RGDfK)₂] that targets integrin $\alpha v \beta 3$. *Bioconjugate Chem.* **2008**, *19*, 1414-22.
51
52
53
54
55
56
57
58
59
60

1
2
3
4
5 (22) Mukhopadhyay, S.; Barnés, C. M.; Haskel, A.; Short, S. M.; Barnes, K. R.; Lippard, S. J.
6
7
8 Conjugated platinum(IV)-peptide complexes for targeting angiogenic tumor vasculature.
9
10 *Bioconjugate Chem.* **2008**, *19*, 39-49.

11
12
13 (23) (a) Dal Pozzo, A.; Ni, M.H.; Esposito, E.; Dallavalle, S.; Musso, L.; Bargiotti, A.; Pisano,
14
15 C.; Vesci, L.; Bucci, F.; Castorina, M.; Fodera, R.; Giannini, G.; Aulicino, C.; Penco, S. Novel
16
17 tumor-targeted RGD peptide-camptothecin conjugates: Synthesis and biological evaluation.
18
19 *Bioorg. Med. Chem. Lett.* **2010**, *18*, 64-72. (b) Alloatti, D.; Giannini, G.; Vesci, L.; Castorina,
20
21 M.; Pisano, C.; Badaloni, E.; Cabri, W. Camptothecins in tumor homing via an RGD sequence
22
23 mimetic. *Bioorg. Med. Chem. Lett.* **2012**, *22*, 6509-6512.
24
25
26

27
28 (24) (a) Chen, X.; Plasencia, C.; Hou, Y.; Neamati, N. Synthesis and biological evaluation of
29
30 dimeric RGD peptide-paclitaxel conjugate as a model for integrin-targeted drug delivery. *J. Med.*
31
32 *Chem.* **2005**, *48*, 1098-106 (corrigendum *J. Med. Chem.*, **2005**, *48*, 5874). (b) Cao, Q.; Li, Z.-B.;
33
34 Chen, K.; Wu, Z.; He, L.; Neamati, N.; Chen, X. Evaluation of biodistribution and anti-tumor
35
36 effect of a dimeric RGD peptide-paclitaxel conjugate in mice with breast cancer. *Eur. J. Nucl.*
37
38 *Med. Mol. Imaging.* **2008**, *35*, 1489-98.
39
40
41

42
43 (25) Ryppa, C.; Mann-Steinberg, H.; Biniossek, M.L.; Satchi-Fainaro, R.; Kratz, F. In vitro and
44
45 in vivo evaluation of a paclitaxel conjugate with the divalent peptide E-[c(RGDfK)₂] that targets
46
47 integrin $\alpha_V\beta_3$. *Int. J. Pharm.* **2009**, *368*, 89-97.
48
49

50
51 (26) Marchini, M.; Mingozi, M.; Colombo, R.; Gennari, C.; Durini, M.; Piarulli, U. Selective
52
53 *O*-acylation of unprotected *N*-benzylserine methyl ester and *O,N*-acyl transfer in the formation of
54
55 cyclo[Asp-Ser] diketopiperazines. *Tetrahedron* **2010**, *66*, 9528-9531.
56
57
58
59
60

1
2
3
4
5 (27) Choi, H.; Aldrich, J. V. Comparison of methods for the Fmoc solid-phase synthesis and
6 cleavage of a peptide containing both tryptophan and arginine. *Int. J. Pept. Protein Res.* **1993**,
7
8 42, 58-63.
9

10
11
12 (28) Deutsch, H. M.; Glinski, J. A.; Hernandez, M.; Haugwitz, R. D.; Narayanan, V. L.;
13 Suffness, M.; Zalkow, L. H. Synthesis of congeners and prodrugs. 3. Water-soluble prodrugs of
14 taxol with potent antitumor activity. *J. Med. Chem.* **1989**, 32, 788-792.
15
16
17

18
19 (29) (a) Buchegger, F.; Kosinski, M.; Viertl, D.; Poitry-Yamate, C.; Baechler, S.; Prior, J.;
20 Tumor localization and mouse-derived dosimetry projection for Ga-68-NODAGA-RGD PET. *J.*
21 *Nucl. Med. Meeting Abstracts* **2011**, 52, 1487. (b) Ye, Y.; Zhu, L.; Ma, Y.; Niu, G.; Chen X.
22 Synthesis and evaluation of new iRGD peptide analogs for tumor optical imaging. *Bioorg. Med.*
23 *Chem. Lett.* **2011**, 21, 1146–1150.
24
25
26
27
28
29
30
31

32
33 (30) Liu, S.; Liu, Z.; Chen, K.; Yan, Y.; Watzlowik, P.; Wester, H. J.; Chin, F. T.; Chen, X.
34 ¹⁸F-Labeled galacto and PEGylated RGD dimers for PET imaging of $\alpha_v\beta_3$ integrin expression.
35 *Mol. Imaging Biol.* **2010**, 12, 530-538.
36
37
38
39

40
41 (31) (a) Fani, M.; Psimadas, D.; Zikos, C.; Xanthopoulos, S.; Loudos, G. K.; Bouziotis, P.;
42 Varvarigou, A. D. Comparative Evaluation of Linear and Cyclic ^{99m}Tc-RGD Peptides for
43 targeting of integrins in tumor angiogenesis. *Anticancer Res.* **2006**, 26, 431-434. (b) Lang, L.; Li,
44 W.; Guo, N.; Ma, Y.; Kiesewetter, D. O.; Niu, G.; Chen, X. Comparison Study of [¹⁸F]FAI-
45 NOTA-PRGD2, [¹⁸F]FPPRGD2, and [⁶⁸Ga]Ga-NOTA-PRGD2 for PET Imaging of U87MG
46 Tumors in Mice. *Bioconjugate Chem.* **2011**, 22, 2415–2422. (c) Li, W.; Lang, L.; Niu, G.; Guo,
47 N.; Ma, Y.; Kiesewetter, D. O.; Shen, B.; Chen, X. *N*-Succinimidyl 4-[¹⁸F]-
48
49
50
51
52
53
54
55
56
57
58
59
60

1
2
3
4
5 fluoromethylbenzoate-labeled dimeric RGD peptide for imaging tumor integrin expression.
6
7
8 *Amino Acids* **2012**, *43*, 1349-1357.

9
10 (32) (a) Janssen, M. L.; Oyen, W. J.; Dijkgraaf, I.; Massuger, L. F.; Frielink, C.; Edwards, D.
11 S.; Rajopadhye, M.; Boonstra, H.; Corstens, F. H.; Boerman, O. C. Tumor targeting with
12 radiolabeled $\alpha_v\beta_3$ integrin binding peptides in a nude mouse model. *Cancer Res.* **2002**, *62*, 6146-
13 6151. (b) Lanzardo, S.; Conti, L.; Brioschi, C.; Bartolomeo, M. P.; Arosio, D.; Belvisi, L.;
14 Manzoni, L.; Maiocchi, A.; Maisano, F.; Forni, G. A new optical imaging probe targeting $\alpha_v\beta_3$
15 integrin in glioblastoma xenografts. *Contrast Media Mol. Imaging* **2011**, *6*, 449–458.

16
17
18 (33) Haubner, R.; Schmitt, W.; Höllzemann, G.; Goodman, S. L.; Jonczyk, A.; Kessler, H.
19 Cyclic RGD Peptides Containing β -Turn Mimetics. *J. Am. Chem. Soc.* **1996**, *118*, 7881-7891.

20
21 (34) Manzoni, L.; Belvisi, L.; Arosio, D.; Civera, M.; Pilkington-Miksa, M.; Potenza, D.;
22 Caprini, A.; Araldi, E. M. V.; Monferrini, E.; Mancino, M.; Podestà, F.; Scolastico, C. Cyclic
23 RGD-including functionalized azabicycloalkane amino acids as potent integrin antagonists for
24 tumor targeting. *ChemMedChem* **2009**, *4*, 615-632, and references cited therein.

25
26 (35) Fu, Y.; Li, S.; Zu, Y.; Yang, G.; Yang, Z.; Luo, M.; Jiang, S.; Wink, M.; Efferth, T.
27 Medicinal chemistry of paclitaxel and its analogues. *Curr. Med. Chem.* **2009**, *16*, 3966-3985.

28
29 (36) Recently, a azabicycloalkane-RGD bound to Paclitaxel via a cleavable diglycolyl ester
30 linker at C2' was reported to provide promising *in vitro* and *in vivo* antitumor activity, see:
31 Pilkington-Miksa, M.; Arosio, D.; Battistini, L.; Belvisi, L.; De Matteo, M.; Vasile, F.; Burreddu,
32 P.; Carta, P.; Rassu, G.; Perego, P.; Carenini, N.; Zunino, F.; De Cesare, M.; Castiglioni, V.;
33 Scanziani, E.; Scolastico, C.; Casiraghi, C.; Zanardi, F.; Manzoni, L. Design, Synthesis and
34
35
36
37
38
39
40
41
42
43
44
45
46
47
48
49
50
51
52
53
54
55
56
57
58
59
60

1
2
3
4
5 Biological Evaluation of Novel cRGD-Paclitaxel Conjugates for Integrin-Assisted Drug
6 Delivery. *Bioconjugate Chem.* **2012**, *23*, 1610-1622.

9
10 (37) (a) Matson, D. R.; Stukenberg, P. T. Spindle poisons and cell fate: a tale of two pathways.
11 *Molecular interventions* **2011**, *11*, 141-150. (b) Portugal, J.; Mandilla, S.; Bataller, M.
12 Mechanisms of drug-induced mitotic catastrophe in cancer cells. *Current Pharmaceutical Design*
13 **2010**, *16*, 69-78; (c) Roninson, I. B.; Broude, E. V.; Chang, B. D. If not apoptosis, then what?
14 Treatment-induced senescence and mitotic catastrophe in tumor cells. *Drug Resistance Updates*
15 **2001**, *4*, 303-313.

16
17 (38) Huang, Y.; Dalton, D. R.; Carroll, P. J. The Efficient, Enantioselective Synthesis of Aza
18 Sugars from Amino Acids. 1. The Polyhydroxylated Pyrrolidines. *J. Org. Chem.* **1997**, *62*, 372-
19 376.

20
21 (39) Webster, K. L.; Maude, A. B.; O'Donnell, M. E.; Mehrotra, A. P.; Gani, D. Design and
22 preparation of serine-threonine protein phosphatase inhibitors based upon the nodularin and
23 microcystin toxin structures. Part 3. *J. Chem. Soc. Perkin Trans. 1* **2001**, 1673-1695.

24
25 (40) Pirrung, M. C.; Shuey, S. W. Photoremovable Protecting groups for phosphorylation of
26 chiral alcohols. Asymmetric synthesis of phosphotriesters of (-)-3',5'-dimethoxybenzoic acid.
27 *J. Org. Chem.* **1994**, *59*, 3890-3897.

28
29 (41) Rosenberg, S. H.; Spina, K. P.; Woods, K. W.; Polakowski, J.; Martin, D. L.; Yao, Z.;
30 Stein, H. H.; Cohen, J.; Barlow, J. L.; Egan D. A.; Tricarico, K. A.; Baker, W. R.; Kleinert, H. D.
31 Studies directed toward the design of orally active renin inhibitors, 1: some factors influencing
32 the absorption of small peptides. *J. Med. Chem.* **1993**, *36*, 449-459.

(42) Gu, K.; Bi, L.; Zhao, M.; Wang, C.; Ju, J.; Peng, S. Toward the development of chemoprevention agents. Part 1: Design, synthesis, and anti-inflammatory activities of a new class of 2,5-disubstituted-dioxacycloalkanes. *Bioorg. Med. Chem.* **2007**, *15*, 6273-6290.

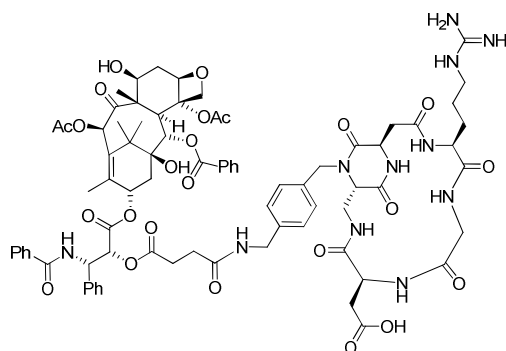
(43) Humphrey, J. M.; Bridges, R. J.; Hart, J. A.; Chamberlin, A. R. 2,3-Pyrrolidinedicarboxylates as Neurotransmitter Conformer Mimics: Enantioselective Synthesis via Chelation-Controlled Enolate Alkylation. *J. Org. Chem.* **1994**, *59*, 2467-2472.

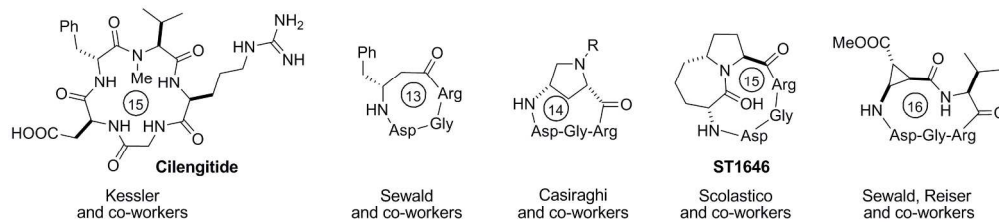
(44) Narukawa, Y.; Juneau, K. N.; Snustad, D.; Miller, D. B.; Hegedus, L. S. Synthesis of optically active β -lactams by the photolytic reaction of imines with optically active chromium carbene complexes. 2. Synthesis of 1-carbacephalothin and 3-ANA relays. *J. Org. Chem.* **1992**, *57*, 5453-5462.

(45) Still, W. C.; Kahn, M.; Mitra, A. Rapid Chromatographic Techniques for Preparative Separation with Moderate Resolution. *J. Org. Chem.* **1978**, *43*, 2923-2925.

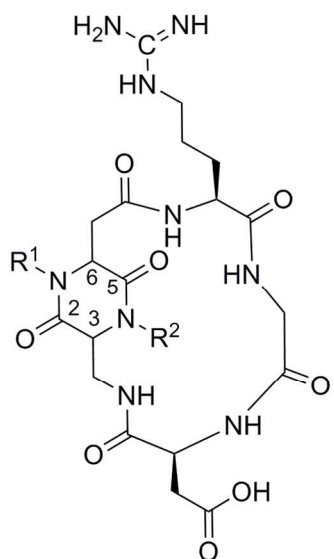
(46) (a) Perego, P.; Romanelli, S.; Carenini, N.; Magnani, I.; Leone, R.; Bonetti, A.; Paolicchi, A.; Zunino, F. Ovarian cancer cisplatin-resistant cell lines: Multiple changes including collateral sensitivity to taxol. *Ann. Oncol.* **1998**, *9*, 1-8. (b) Perego, P.; Giarola, M.; Righetti, S. C.; Supino, R.; Caserini, C.; Delia, D.; Pierotti, M. A.; Miyashita, T.; Reed, J. C.; Zunino, F. Association between cisplatin resistance and mutation of p53 gene and reduced bax expression in ovarian carcinoma cell systems. *Cancer Res.* **1996**, *56*, 556-562.

Table of Contents graphic



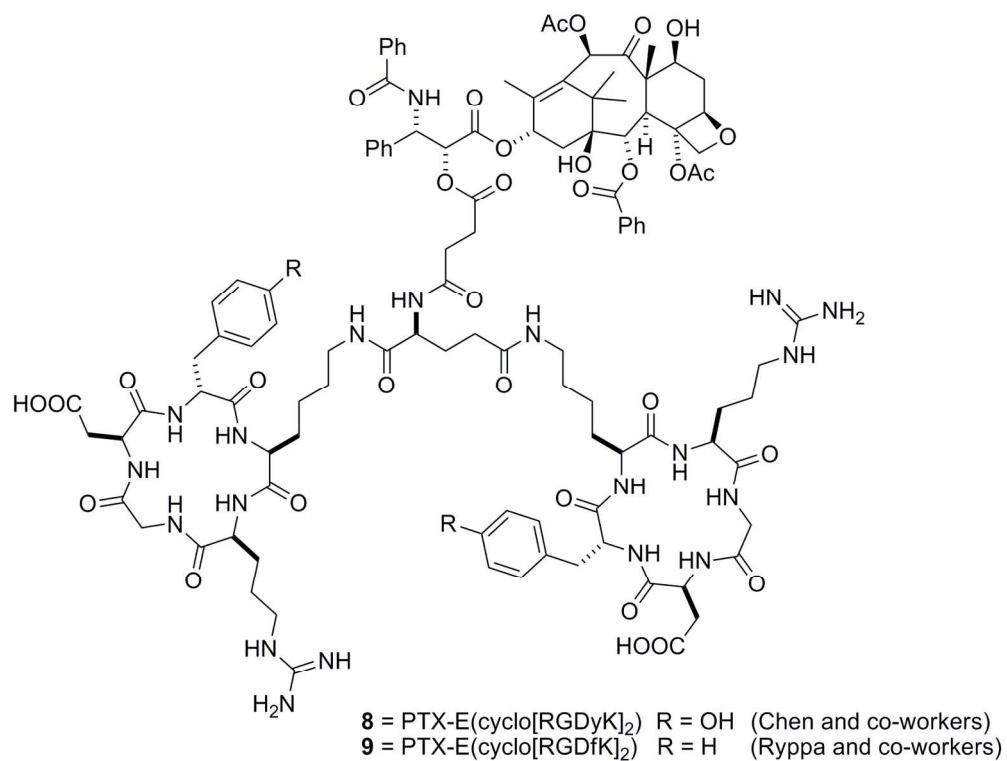


220x48mm (300 x 300 DPI)

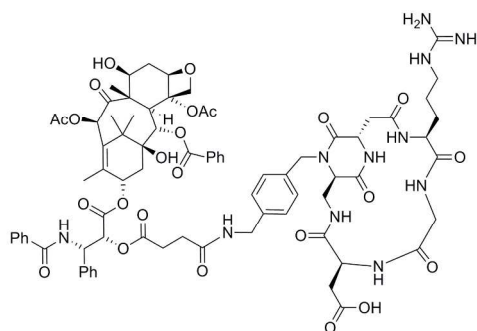


- 1** = *cyclo*[DKP-1-RGD] = 3*S*, 6*S*, R¹=H, R²=Bn
2 = *cyclo*[DKP-2-RGD] = 3*R*, 6*S*, R¹=H, R²=Bn
3 = *cyclo*[DKP-3-RGD] = 3*S*, 6*R*, R¹=H, R²=Bn
4 = *cyclo*[DKP-4-RGD] = 3*R*, 6*S*, R¹=Bn, R²=H
5 = *cyclo*[DKP-5-RGD] = 3*R*, 6*S*, R¹=Bn, R²=Bn
6 = *cyclo*[DKP-6-RGD] = 3*S*, 6*R*, R¹=Bn, R²=H
7a = *cyclo*[DKP-7-RGD]^a = 3*S*, 6*R*, R¹=Bn, R²=Bn
7b = *cyclo*[DKP-7-RGD]^a = 3*S*, 6*R*, R¹=Bn, R²=Bn

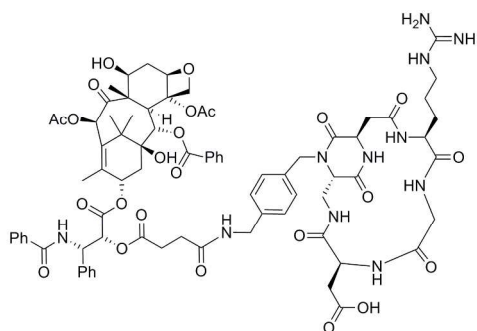
130x72mm (300 x 300 DPI)



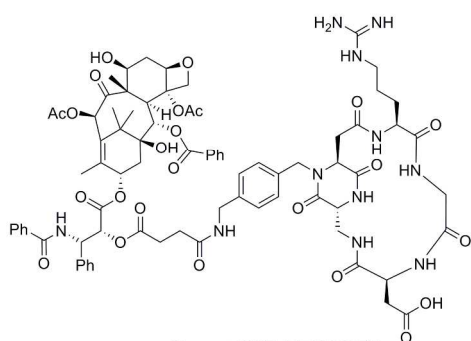
149x112mm (300 x 300 DPI)



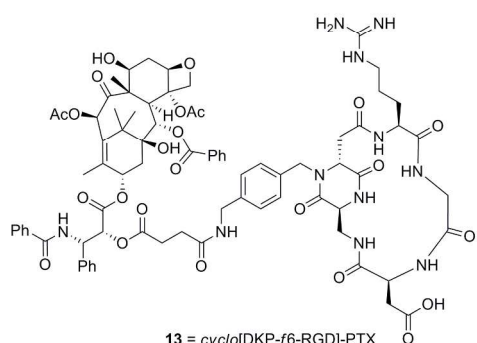
10 = *cyclo*[DKP-f2-RGD]-PTX



11 = *cyclo*[DKP-f3-RGD]-PTX



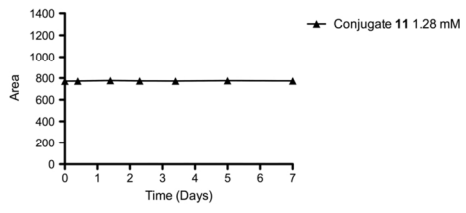
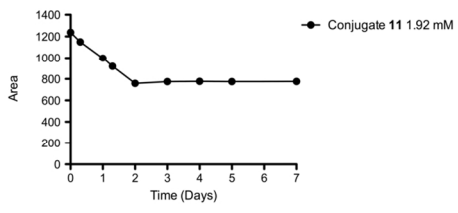
12 = *cyclo*[DKP-f4-RGD]-PTX



13 = *cyclo*[DKP-f6-RGD]-PTX

223x166mm (300 x 300 DPI)

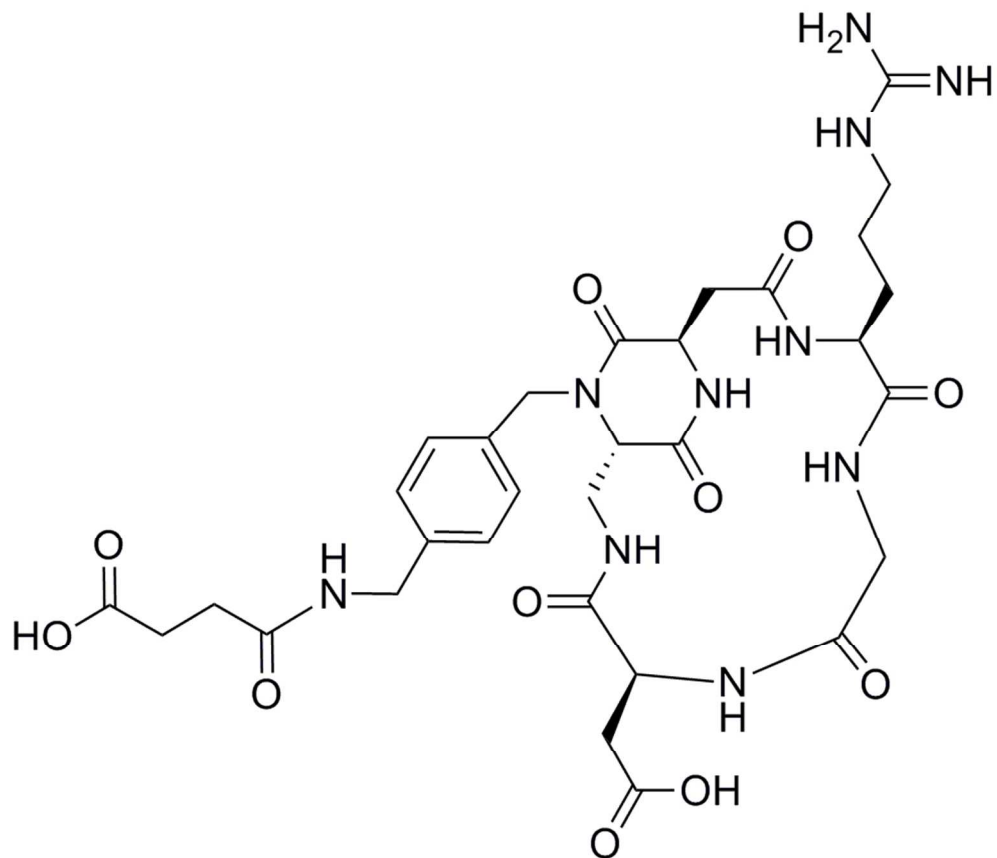
1
2
3
4
5
6
7
8
9
10
11
12
13
14
15
16
17
18
19
20
21
22
23
24
25
26
27
28
29
30
31
32
33
34
35
36
37
38
39
40
41
42
43
44
45
46
47
48
49
50
51
52
53
54
55
56
57
58
59
60



63x16mm (600 x 600 DPI)

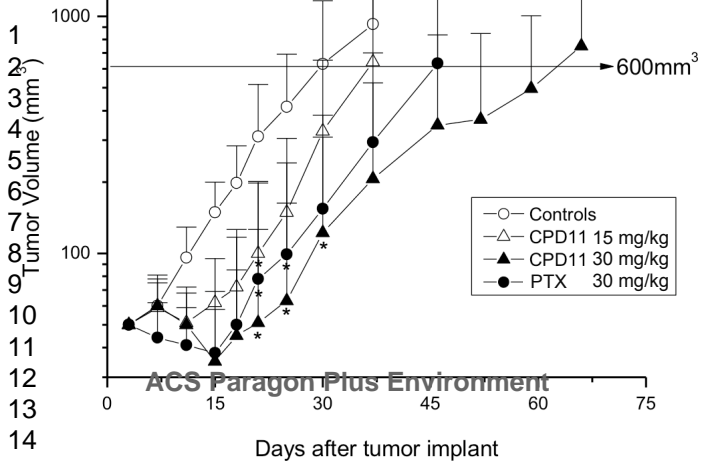
Unable to Convert Image

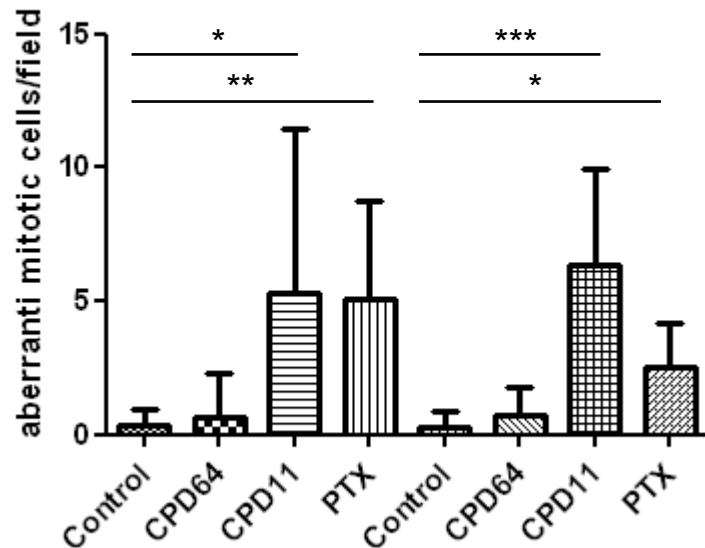
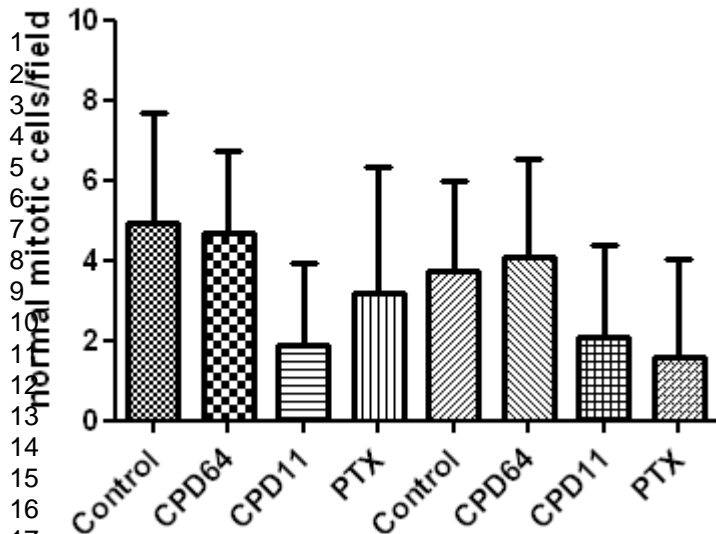
The dimensions of this image (in pixels) are too large to be converted. For this image to convert, the total number of pixels (height x width) must be less than 40,000,000 (40 megapixels).



68 = *cyclo*[DKP-*f*3-RGD]-hemisuccinamide

84x80mm (300 x 300 DPI)





1
2
3
4
5
6
7
8
9
10
11
12

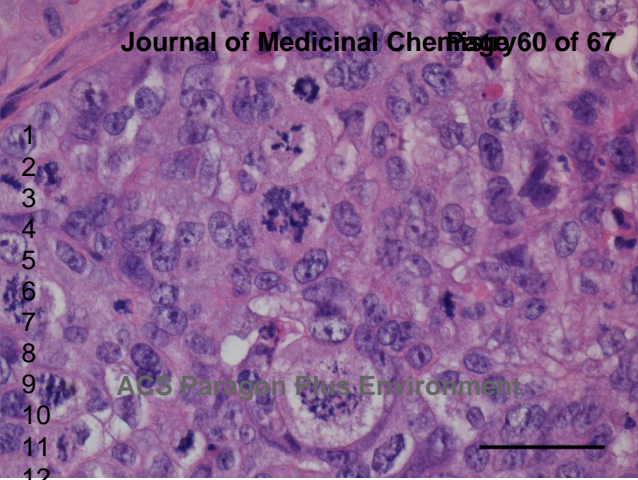
ACS Paragon Plus Environment



1
2
3
4
5
6
7
8
9
10
11
12

ACS Paragon Plus Environment





1

2

3

4

5

6

7

8

9

10

11

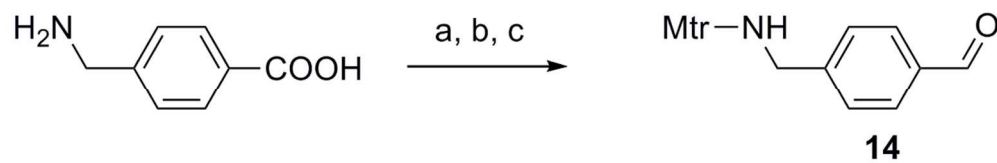
12

ACS Paragon Plus Environment

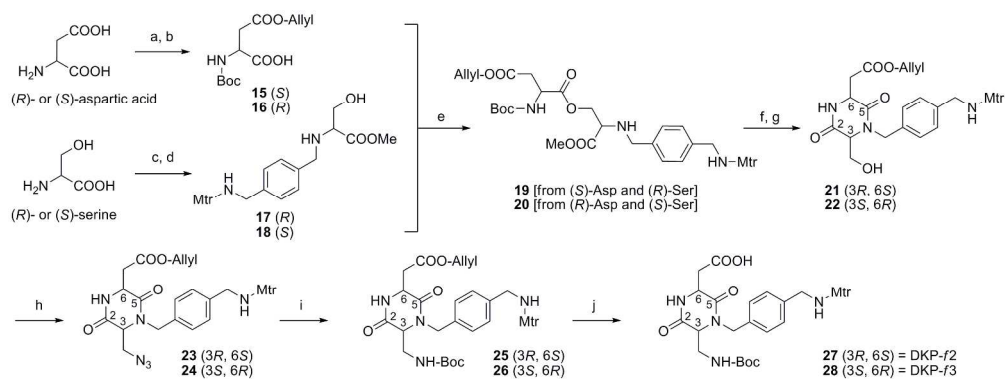
1
2
3
4
5
6
7
8
9
10
11
12

ACS Paragon Plus Environment

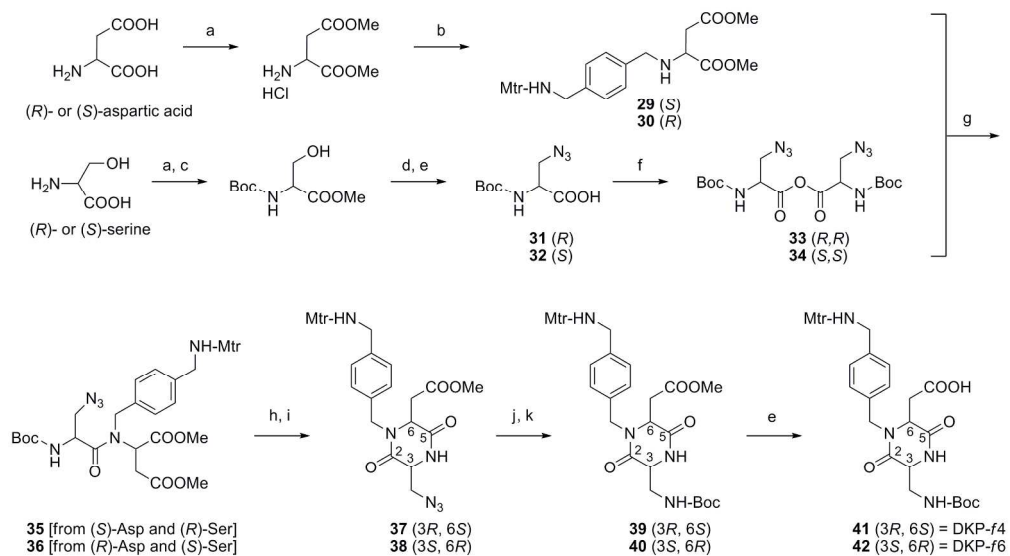


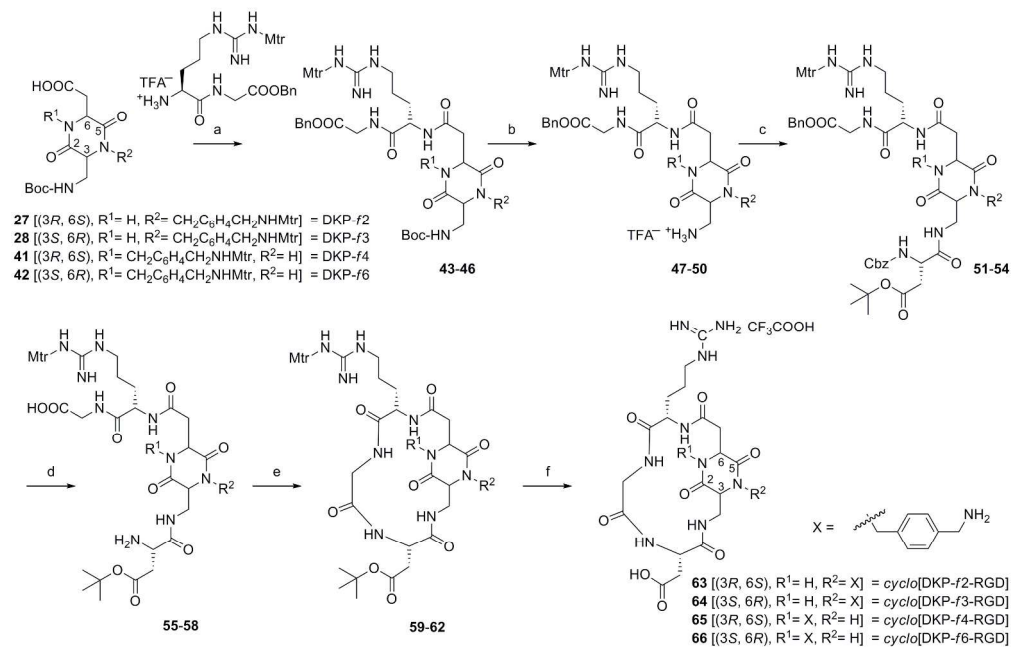


106x17mm (300 x 300 DPI)

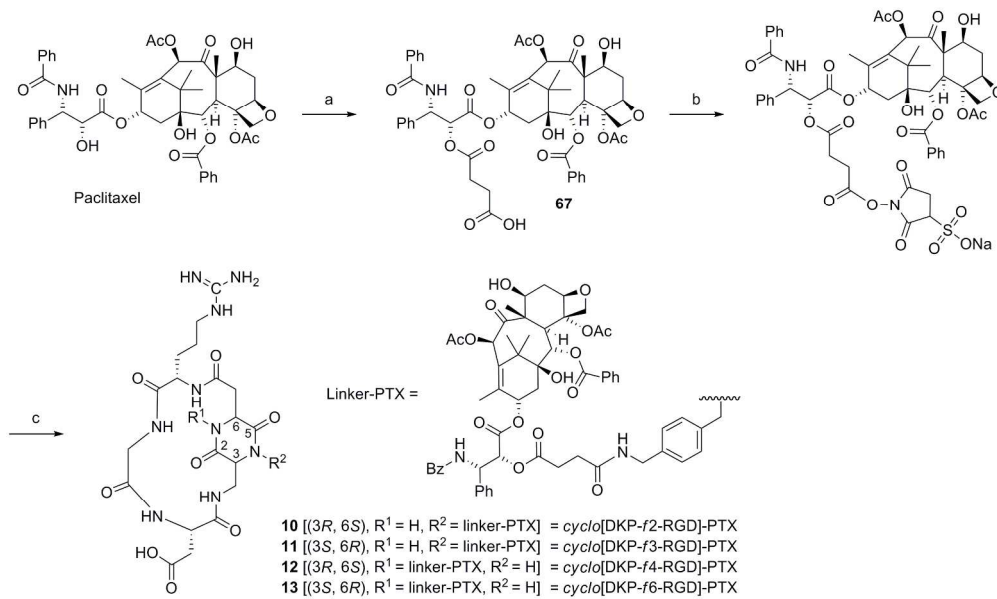


251x93mm (300 x 300 DPI)

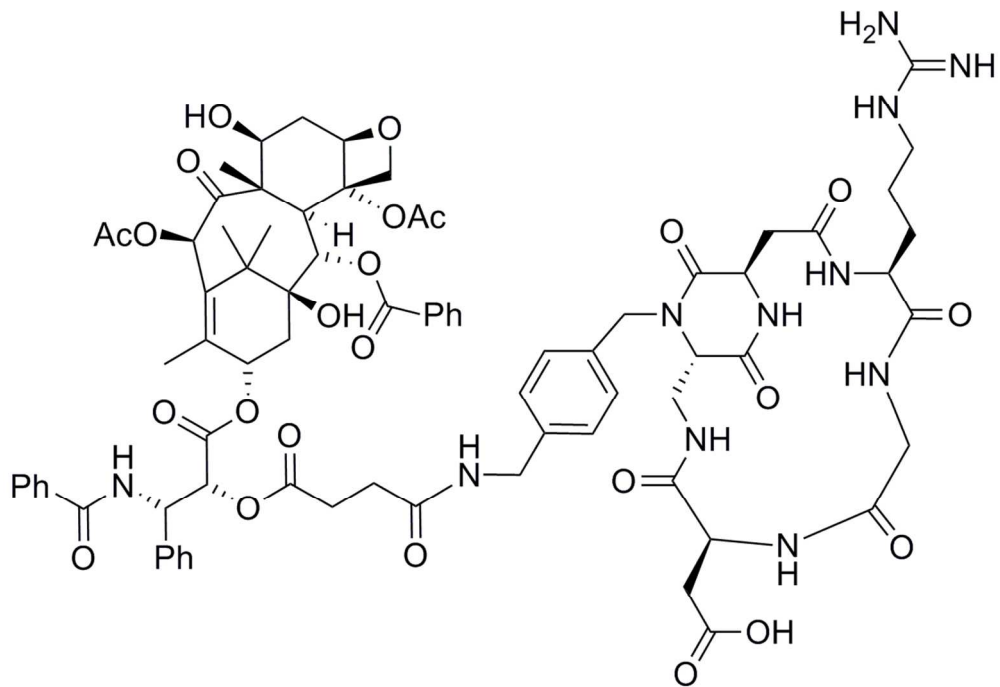




249x159mm (300 x 300 DPI)



224x132mm (300 x 300 DPI)



105x72mm (300 x 300 DPI)